Electronic Supplementary Material (ESI) for ChemComm.


# Cross-dehydrogenative C($sp^3$)-C($sp^3$) coupling *via* C-H activation using magnetically retrievable ruthenium-based photoredox nanocatalyst under aerobic conditions

Pooja Rana,[a] Rashmi Gaur,[a] Radhika Gupta,[a] Gunjan Arora,[a] A. Jayashree,[b] and Rakesh Kumar Sharma*[a]

[a.] Green Chemistry Network Centre, Department of Chemistry, University of Delhi, New Delhi-110007, India; Tel: 011-276666250; Email: rksharmagreenchem@hotmail.com

[b.] Centre for Chemical Sciences & Technology, IST, Jawaharlal Nehru Technological University Hyderabad 500085, India.

**In the present work, we report the fabrication of a highly versatile ruthenium-based magnetically recoverable photoredox nanocatalyst with large surface area. This visible light harvesting nanocatalyst was effectively used for cross-dehydrogenative coupling *via* C-H activation between tertiary amines and various carbon nucleophiles with high regioselectivity to afford the C-C coupled products in good to excellent yield using air as an oxidant under ambient conditions. The Ru-based catalyst was found to be a potential candidate from the economical and environmental perspective due to magnetic recoverability and reusability.**

**Table of Contents**

## General Information

*Materials Synthesis*. Unless otherwise indicated, all reagents were commercially purchased and used without further purification. Ferric sulphate hydrate and ferrous sulphate heptahydrate were purchased from Central Drug house and Thomas Bakers, respectively. Solvents (Methanol, Ethyl acetate, Petroleum ether and MeCN) used for preparative liquid chromatography were of technical grade and used after distillation in a rotary evaporator. All the photochemical reactions were carried out under air atmosphere unless otherwise indicated. Some substrates and their precursors including DAFO and *N*-aryl-tetrahydroisoquinolines[1] were prepared according to their reported procedures.

*Material Characterisation.* The fabricated Ru@DAFO@ASMNPs were characterised by using Fourier transform-infrared spectroscopy (FT-IR), powder X-ray diffraction (PXRD), UV-Vis spectroscopy, field emission-scanning electron microscopy (FE-SEM), high resolution-transmission electron microscopy (HR-TEM), vibrating sample magnetometery (VSM), Brunauer-Emmett-Teller analysis (BET), inductively coupled-plasma optical emission spectrometry (ICP-OES), X-ray photoelectron spectroscopy (XPS), energy-dispersive X-ray spectroscopy (EDS), energy-dispersive X-ray fluorescence (ED-XRF), high resolution-mass spectroscopy (HR-MS), gas chromatography-mass spectrometry (GC-MS) and nuclear magnetic resonance spectroscopy (NMR). The infrared spectra were recorded from 4000 to 400 $cm^{-1}$ on PerkinElmer Spectrum 2000 using KBr pallet method. PXRD patterns were recorded on a Rigaku Cu ($K_\alpha$) diffractogram at a scan rate of 4 degree per min and 2θ range of 2-80 degree for determining the crystallinity. UV/Vis spectra have been carried out on a Thermo Scientific absorption spectrophotometer within the wavelength range 200-900 nm. FE-SEM was performed on a Tescan MIRA3 FE-SEM microscope. SEM analysis was carried out using gold sputtered nanoparticles over a carbon tape. TEM images were collected using a FEI TECHNAI $G^2$ T20 transmission electron microscope operated at 200 KV. The samples were prepared by drop casting a sonicated ethanol suspension of the desired nanoparticles over a copper grid with an amorphous carbon film. Elemental analysis of the catalyst was carried out on a Ametek EDAX system. Brunauer-Emmett-Teller (BET) method was acquired using a ASI-CT-11 Quantachrome instrument at a degassing temperature of 180 °C to determine the specific surface area, pore volume and pore size distribution. Metal content of the catalyst was measured on Perkin Elmer Avio ICP-OES System. Magnetization was recorded using a vibrating sample magnetometer (EV-9, Microsense, ADE) in the range of -10000 Oe to 10000 Oe. The optimization of the reaction was carried out using an Agilent gas chromatograph (6850 GC) having a HP-5MS capillary column (stationary phase: 5% phenyl methyl siloxane; column length: 30 m; internal diameter: 0.25 mm; film thickness: 0.25 µm) and a quadrupole mass filter equipped 5975C mass selective detector (MSD) using helium as a carrier gas. $^1$H NMR (400 MHz) and $^{13}$C NMR (100 MHz) spectra were recorded using a JEOL JNM-EXCP 400. Chemical shifts (δ) are recorded in ppm downfield relative to tetramethylsilane (served as internal standard) and are referenced to the carbon resonance of the solvent. Abbreviations used to express the multiplicities/signal couplings are: singlet (s), doublet (d), triplet (t) and multiplet (m). High-resolution mass spectra were recorded on electrospray mass spectrometer using Agilent G6530AA (LC-HRMS-Q-TOF). All the reactions were monitored by thin layer chromatography using Merck silica gel plates 60 F254 and visualised under UV light.

Three different lamps have been used:
Lamp 1: 10 W blue LEDs
Lamp 2: 12 W Philips UV-A lamp
Lamp 3: 12 W Philips Fluorescent tube

## Experimental Section

***Synthesis of photocatalyst***

**Preparation of nanocrystalline magnetic particles[2]**

In a conventional experiment, $FeSO_4.7H_2O$ (4.2 g) and $Fe_2(SO_4)_3$ (6.0 g) were added to 250 mL double distilled water and stirred untill a clear orange solution was observed. Then, ammonium hydroxide (25%) was added drop wise to adjust the pH 10. The reaction mixture was vigorously stirred for 1 hour at a temperature of 60 °C. The iron based magnetic nanoparticles were separated *via* applying an external magnet which were further washed and dried for 5 hour at 50 °C in vacuum. The obtained MNPs were finely crushed for the further reaction steps.

**Preparation of silica-coated magnetic nanoparticles[3, 4]**

The iron based magnetic nanoparticles were silica coated using tetraethyl orthosilicate (TEOS). Initially, MNPs (0.5 g) were activated *via* treating with 0.1 M HCl (2.2 mL) and 4:1 v/v ethanol-water (250 mL) mixture was added. The reaction mixture was sonicated for 30 minutes for uniform dispersion of MNPs. In the resultant solution, 25% $NH_4OH$ solution (5 mL) and TEOS (1 mL) were added dropwise and left for stirring at 60 °C. The silica-coated magnetic nanoparticles were subsequently separated *via* external magnet and dried in oven at 60 °C.

**Preparation of APTES functionalized silica-coated magnetic nanoparticles[5]**

SMNPs were amine functionalized using APTES. SMNPs (0.2 g) were added to a solution of APTES (1 mL) in 200 mL ethanol. The mixture was sonicated for 15 minutes and stirred for 6 hours at 60 °C. Then, resultant amine functionalized SMNPs were magnetically separated and washed several times with ethanol and dried in vacuum oven.

**Preparation of DAFO@ASMNPs**

DAFO was synthesised *via* $KMnO_4$ catalysed reaction of phenanthroline with KOH in hot boiling water.[6] The synthesised DAFO was immobilised over ASMNPs *via* Schiff base reaction. The grafting procedure is quite simple which can be performed by refluxing 2 g of ASMNPs with 4 mmol DAFO in 250 mL ethanol for 3 hour. The modified ASMNPs were collected, washed and dried in vacuum oven.

**Preparation of Ru@DAFO@ASMNPs**

The Ru based photocatalyst was synthesised by dispersing the DAFO@ASMNPs (1 g) in dry ethanol (100 mL). Oven dried $RuCl_3$ (200 mg) and sodium hypophosphite (190 mg) were added to the reaction mixture and further refluxed for 5 hours. After completion of the reaction the desired catalyst was magnetically separated, washed with ethanol and dried.

**a) MNPs** **b) SMNPs** **c) Ru@DAFO@ASMNPs**

**Images of fabricated a) MNPs, b) SMNPs and c) Ru@DAFO@ASMNPs.**

**Preparation of homogeneous $[Ru(DAFO)_3]^{2+}$ complex**

The $[Ru(DAFO)_3]^{2+}$ catalyst was fabricated *via* standard protocol.[7] Initially, the synthesised DAFO ligand (546 mg, 3 mmol), sodium hypophosphite ($NaH_2PO_2$, 0.132 g, 1.5 mmol) and oven dried $RuCl_3$ (0.207 g, 1 mmol) were added in dry EtOH (50 mL) and refluxed for 3 h. After completion of the reaction, the solvent was dried using rotary evaporatory, purified by column chromatography and characterised by HR-MS. (**Figure S2a**)

**General procedure for preparation of Mannich reaction products**

A schlenk tube was charged with Ru@DAFO@ASMNPs (35 mg), *N*-aryl-tetrahydroisoquinoline (1 mmol), L-Proline (10 mol%), ketone (10 eq) and 2 mL acetonitrile. The reaction mixture was sonicated for 15 minutes. Afterwards, the reaction mixture was stirred at room temperature and irradiated with 10 W blue LED source by keeping at a distance of 5 cm. The progress of the reaction was monitored *via* TLC. After completion of the reaction, the catalyst was separated *via* external magnet and the solvent was dried using rotary evaporator. The resulting residue was purified using silica column chromatography using ethyl acetate and hexane (1:9).

**General procedure for preparation of nitro Mannich reaction products**

*N*-aryl-tetrahydroisoquinoline (1 mmol), nitroalkane (10 eq), Ru@DAFO@ASMNPs (35 mg) and 1 mL methanol were added and sonicated for 15 minutes in a schlenk tube. Afterwards, the reaction mixture was stirred at room temperature and irradiated with 10 W blue LED source by keeping at a distance of 5 cm. The reaction was monitored *via* TLC. After completion of the reaction, the catalyst was separated *via* external magnet and the solvent was dried using rotary evaporator. The resulting residue was purified using silica column chromatography using ethyl acetate and hexane (1:9).

## Result and discussion

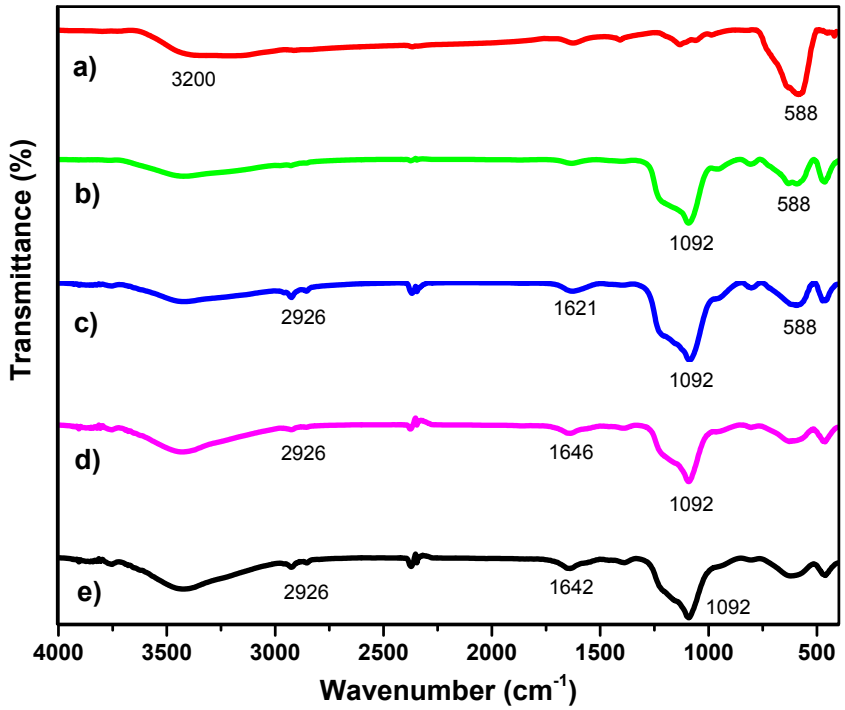


Figure S1 FT-IR spectra of: a) MNPs, b) SMNPs, c) ASMNPs, d) DAFO@ASMNPs and e) Ru@DAFO@ASMNPs.

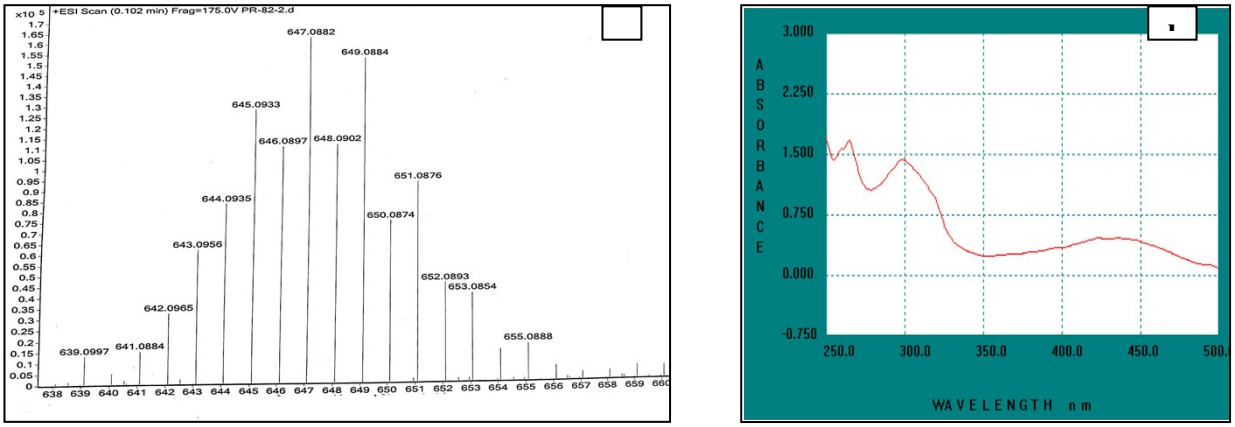


Figure S2 a) ESI mass spectrum and b) UV-Vis spectrum of homogeneous $[Ru(DAFO)_3]^{2+}$ catalyst.

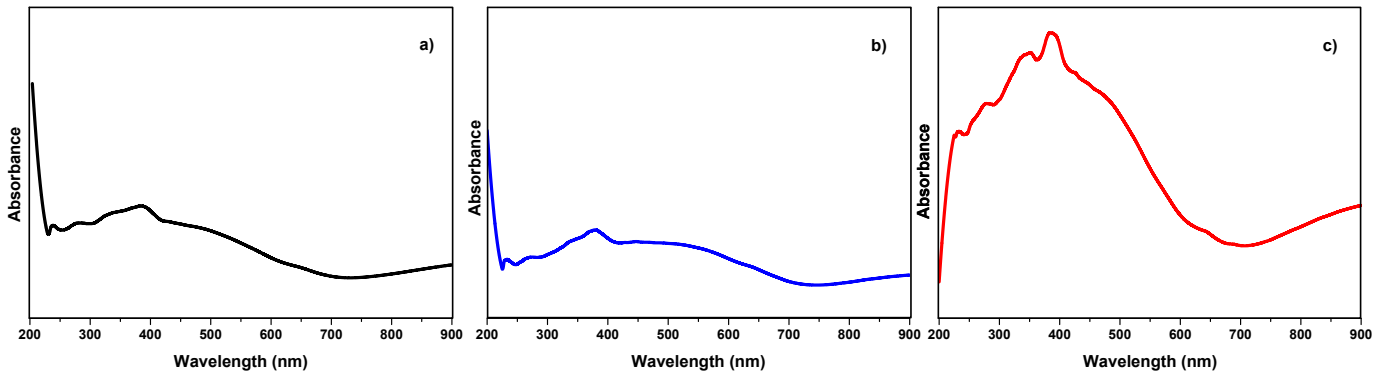


**Figure S3 UV-Vis absorption spectra of: a) MNPs, b) SMNPs and c) Ru@DAFO@ASMNPs.**

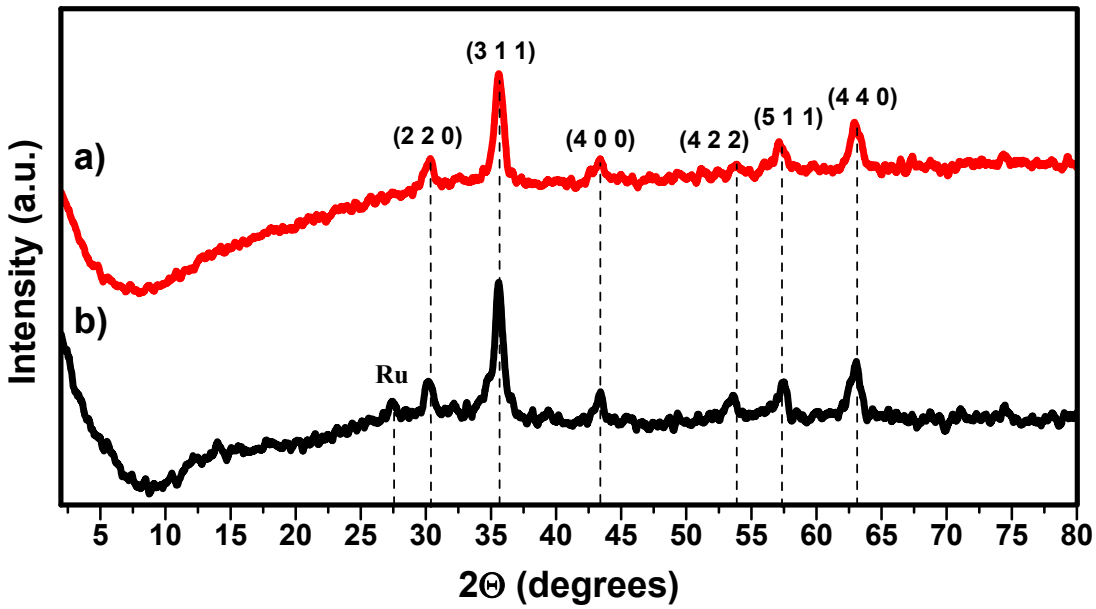


**Figure S4 PXRD pattern of: a) MNPs and b) Ru@DAFO@ASMNPs.**

The spectrum (**Figure S4a**) shows strong characteristic Bragg's diffraction peaks at 2θ of 30.4°, 35.67°, 43.55°, 54.00°, 57.29° and 63.16° which corresponds to (2 2 0), (3 1 1), (4 0 0), (4 2 2), (5 1 1) and (4 4 0) crystal planes respectively and match perfectly with the inverse spinel $Fe_3O_4$ phase (JCPDS card 19-629).[4]

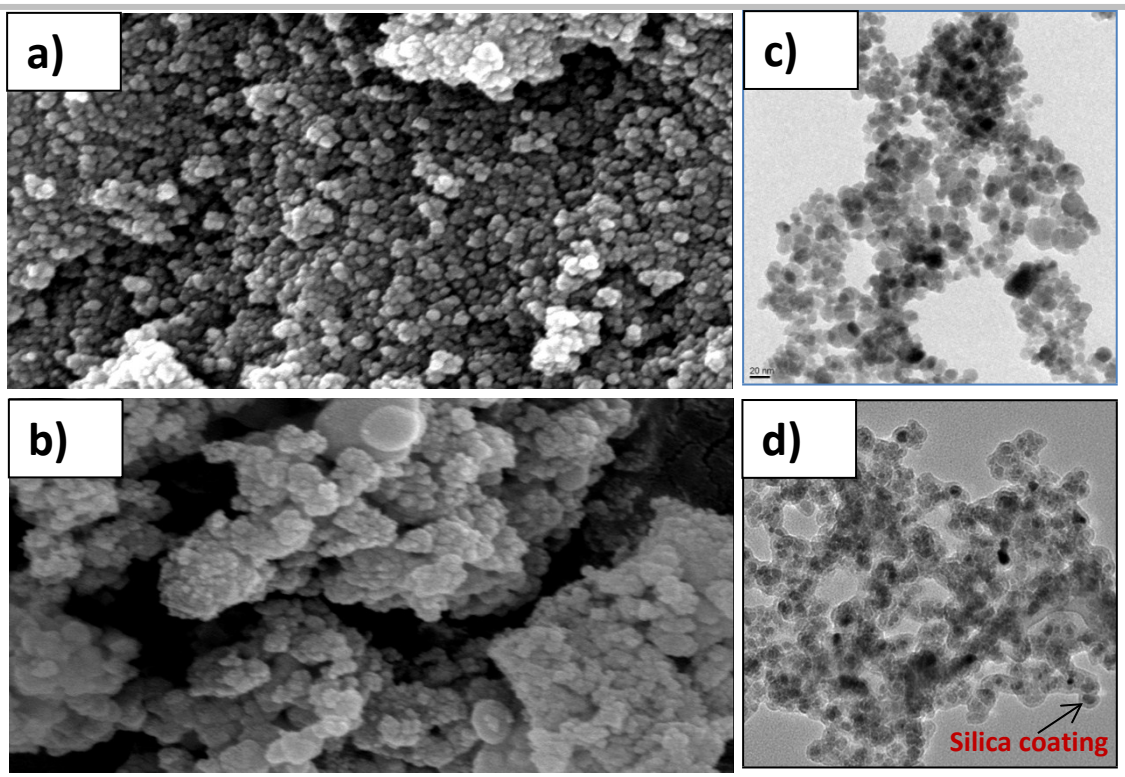


**Figure S5 FE-SEM images of: a) MNPs and b) SMNPs, TEM images of: c) MNPs; d) SMNPs.**

FE-SEM and TEM images of MNPs and SMNPs catalyst reveal that they are spherical in shape. TEM images also manifest that MNPs have an average diameter of 11 nm and SMNPs have a silica coating of about 6 nm in thickness over MNPs. (**Figure S5**)

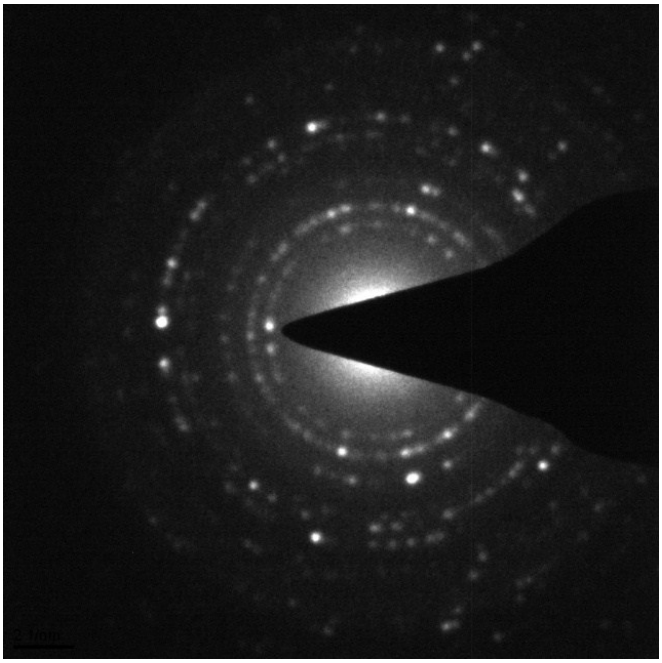

**Figure S6 Selected area electronic diffraction (SAED) pattern of MNPs.**

The selected area electronic diffraction (SAED) pattern of MNPs indicates their polycrystalline nature (**Figure S6**).

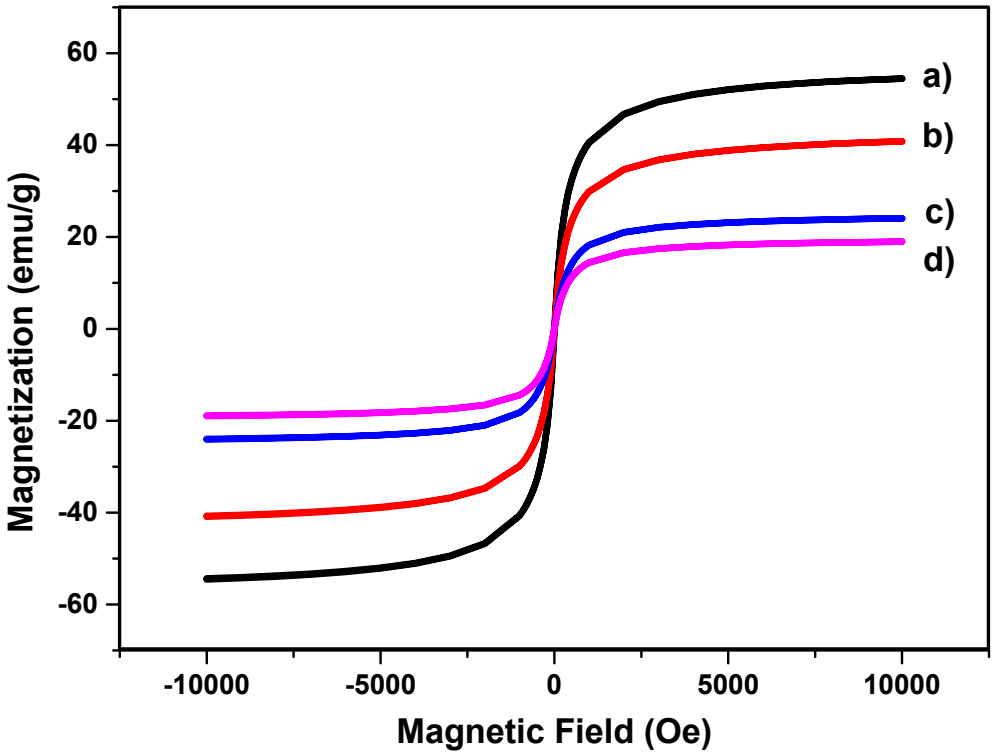


**Figure S7 Magnetization curves of: a) MNPs, b) SMNPs, c) fresh Ru@DAFO@ASMNPs catalyst and d) Recovered Ru@DAFO@ASMNPs catalyst after six runs.**

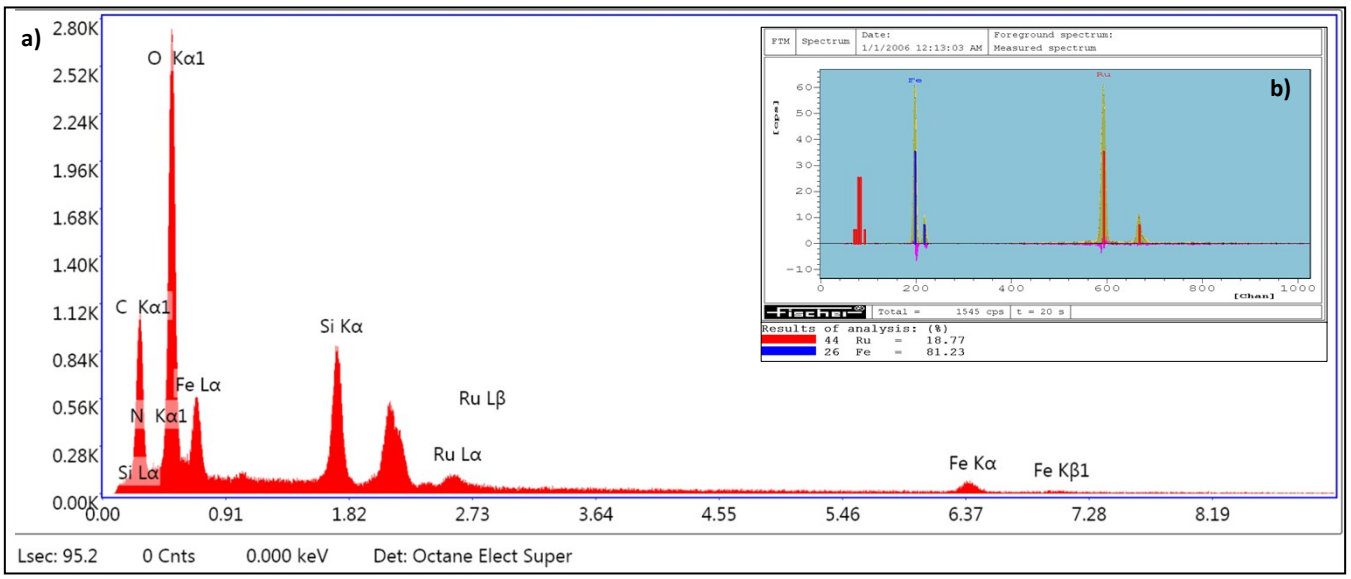


**Figure S8 a) EDS pattern and b) ED-XRF pattern of Ru@DAFO@ASMNPs.**

EDS analysis validate the presence of Fe, Si, C, N, O and Ru in Ru@DAFO@ASMNPs which corresponds to the presence of magnetic core, silica coat, amine group and Ru metal in the final catalyst (**Figure S8**).

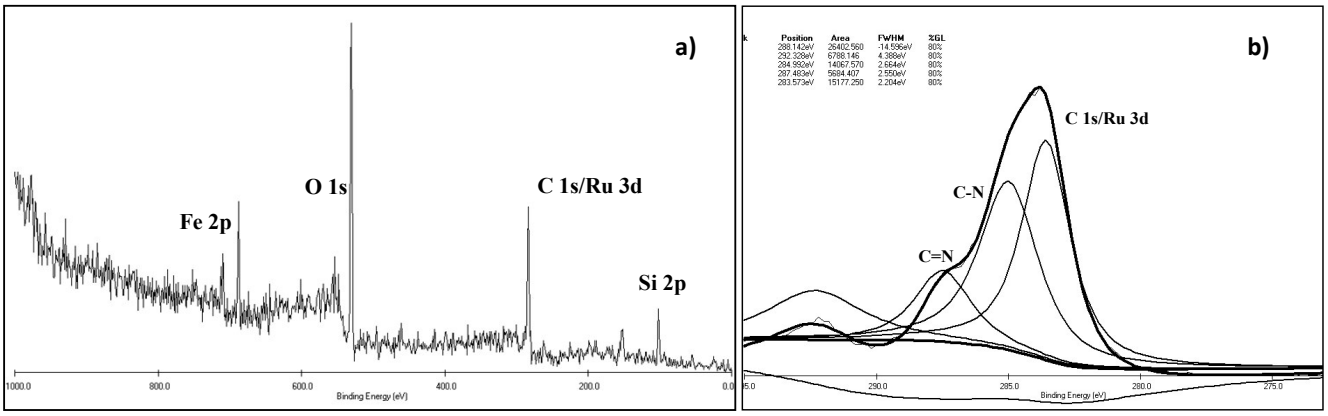


**Figure S9 XPS survey spectra of Ru@DAFO@ASMNPs catalyst: a) Survey scan and b) Ru(3d).**

While, in XPS analysis, the peak due to ruthenium could not be detected that is probably due to the lower loading of ruthenium (in comparison to other metals) or overlapping with C1s peak (**Figure S9**).[8]

## Proposed mechanism of the Photoredox catalysis.

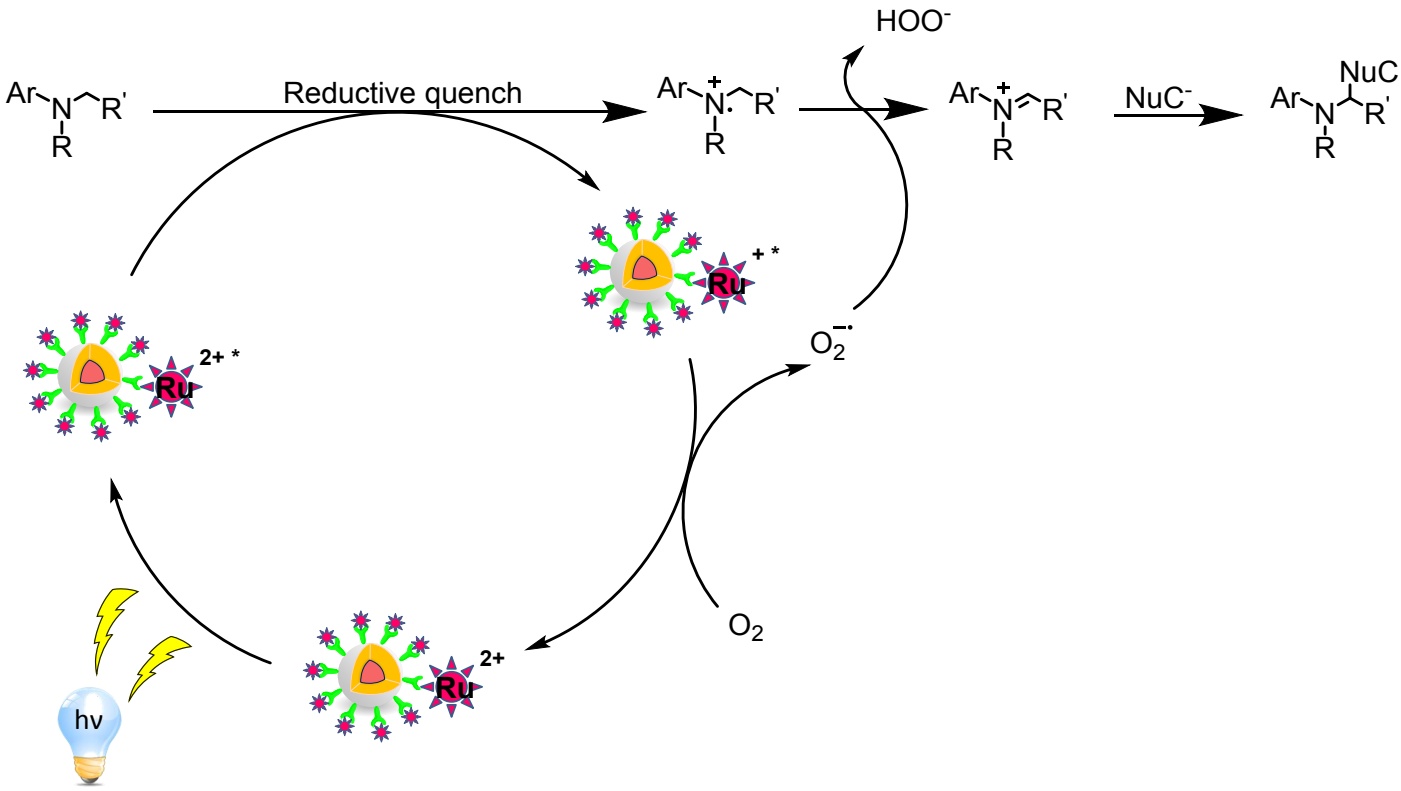


**Scheme S1 Proposed mechanism for cross-dehydrogenative coupling (CDC) reaction using Ru@DAFO@ASMNPs.**

## Tables

**Table S1 Optimization and control experiments for Mannich reaction.**[a]

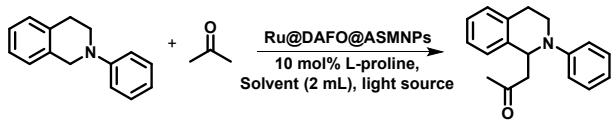


| Entry | Catalyst (mg) | Solvents | Light source | % Yield[b] |
|---|---|---|---|---|
| **i** | 25 | $H_2O$ | 12 W Fluorescent | 75 |
| **ii** | 25 | MeOH | 12 W Fluorescent | 66.8 |
| **iii** | 25 | EtOH | 12 W Fluorescent | 74 |
| **iv** | 25 | MeCN | 12 W Fluorescent | 77 |
| **v** | 25 | MeCN | 10 W Blue | 80 |
| **vi** | 25 | MeCN | 12 W UV light | 59 |
| **vii** | 25 | MeCN | Dark | Trace |
| **viii** | - | MeCN | 10 W Blue | Trace |
| **ix**[c] | 25 | MeCN | 10 W Blue | Trace |
| **x** | - | MeCN | Dark | Nil |
| **xi**[d] | 25 | MeCN | 10 W Blue | 24 |
| **xii** | 15 | MeCN | 10 W Blue | 57 |
| **xiii** | **35** | **MeCN** | **10 W Blue** | **88** |
| **xiv** | 45 | MeCN | 10 W Blue | 89 |

[a]*Reaction conditions*: 1 mmol *N*-phenyl-tetrahydroisoquinoline, 10 eq. acetone, 10 mol% L-Proline, 2 mL solvent, room temperature, 24 h, air. [b]GC-MS yield, [c]$N_2$ atmosphere, [d]No L-Proline.

## TOF

**Table S2 TOF for Mannich reaction.**[a]

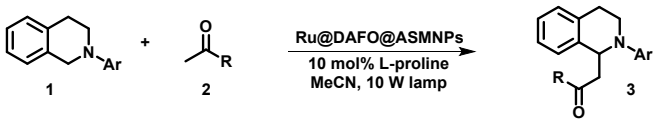


| Entry | Ar | R | Time (h) | (Product, 3) | TOF ($h^{-1}$) |
|---|---|---|---|---|---|
| **i** | Ph | $CH_3$ | 24 | **3a** | 7.8 |
| **ii** | Ph | $CH_2CH_3$ | 20 | **3b** | 9.97 |
| **iii** | Ph | $-CH_2(CH_2)_4-$ | 24 | **3c** | 6.51 |
| **iv** | 4-$CH_3$-Ph | $CH_3$ | 15 | **3d** | 11.94 |
| **v** | 4-$CH_3$-Ph | $CH_2CH_3$ | 24 | **3e** | 7.08 |

| | | | | | |
|---|---|---|---|---|---|
| **vi** | 4-$OCH_3$-Ph | $CH_3$ | 15 | **3f** | 13.15 |
| **vii** | 4-$OCH_3$-Ph | $CH_2CH_3$ | 20 | **3g** | 9.52 |
| **viii** | 4-Cl-Ph | $CH_3$ | 24 | **3h** | 8.03 |
| **ix** | 4-Cl-Ph | $CH_2CH_3$ | 24 | **3i** | 7.74 |
| **x** | Ph | $CH_2CH(CH_3)_2$ | 18 | **3j** | 10.33 |
| **xi** | Ph | Ph | 20 | **3k** | 9.07 |

[a]*Reaction conditions*: 1 mmol *N*-aryl-tetrahydroisoquinolines, 10 eq. ketone, 10 mol% L-Proline, 35 mg Ru@DAFO@ASMNPs, 2 mL MeCN, room temperature, 10 W blue light, air. [b] TON is the number of moles of the product per mole of the catalyst and TOF = TON per hour.

**Table S3 TOF for Nitro-Mannich Reaction.**[a]

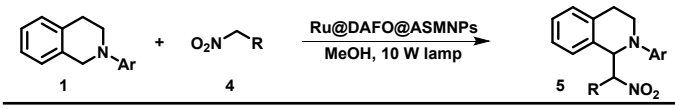


1 4 5

| Entry | Ar | R | Time (h) | Product (5) | TOF ($h^{-1}$) |
|---|---|---|---|---|---|
| **i** | Ph | H | 12 | **5a** | 16.62 |
| **ii** | 4-$CH_3$-Ph | H | 12 | **5b** | 16.81 |
| **iii** | 4-$CH_3$-Ph | $CH_3$ | 12 | **5c** | 15.49 |
| **iv** | Ph | $CH_3$ | 24 | **5d** | 7.36 |
| **v** | 4-$OCH_3$-Ph | H | 18 | **5e** | 9.07 |
| **vi** | 4-Cl-Ph | H | 30 | **5f** | 6.04 |

[a]*Reaction conditions*: 1 mmol *N*-aryl-tetrahydroisoquinolines, 10 eq. nitroalkane, 35 mg Ru@DAFO@ASMNPs, 1 mL MeOH, room temperature, 10 W blue light, air. [b] TON is the number of moles of the product per mole of the catalyst and TOF = TON per hour.

## Reusability test

In the meantime, the recyclability of Ru@DAFO@ASMNPs was also tested which shows that the catalyst can effectively reused upto six runs without any significant change in the percentage yield (**Figure S10**). The recyclability of the catalyst was analyzed with the model reaction of *N*-Phenyl-tetrahydroisoquinoline and acetone under optimized reaction conditions. After completion of reaction, the catalyst was collected *via* external magnet, washed with ethanol and dried in vacuo overnight prior to use. The catalyst was successfully recycled and reused upto six consecutive runs without any significant loss of catalytic activity.

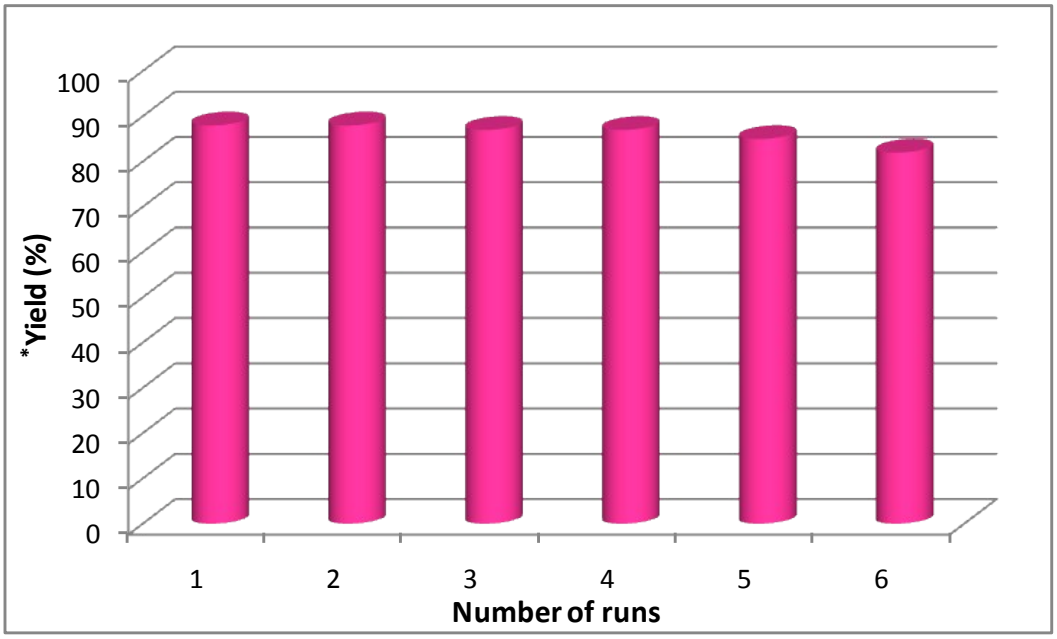


**Figure S10 Reusability test.**

*GC-MS yield.

## Leaching test

In order to investigate the heterogeneous nature of the fabricated Ru@DAFO@ASMNPs catalyst, leaching test was carried out for Mannich reaction between *N*-phenyl-tetrahydroisoquinoline and acetone in the optimized reaction conditions. After 5 hour, catalyst was magnetically separated from the reaction mixture and only 40% conversion was achieved (confirmed by GC-MS). Furthermore, exposing the reaction mixture with light and continuous stirring does not show any significant conversion (42%). It signifies the truly heterogeneous nature of Ru-based nano photocatalyst which has been strongly anchored over the magnetic support. This proves that only negligible leaching of Ru took place in the reaction mixture during the course of the catalytic reaction which was further confirmed by ICP-OES analysis.

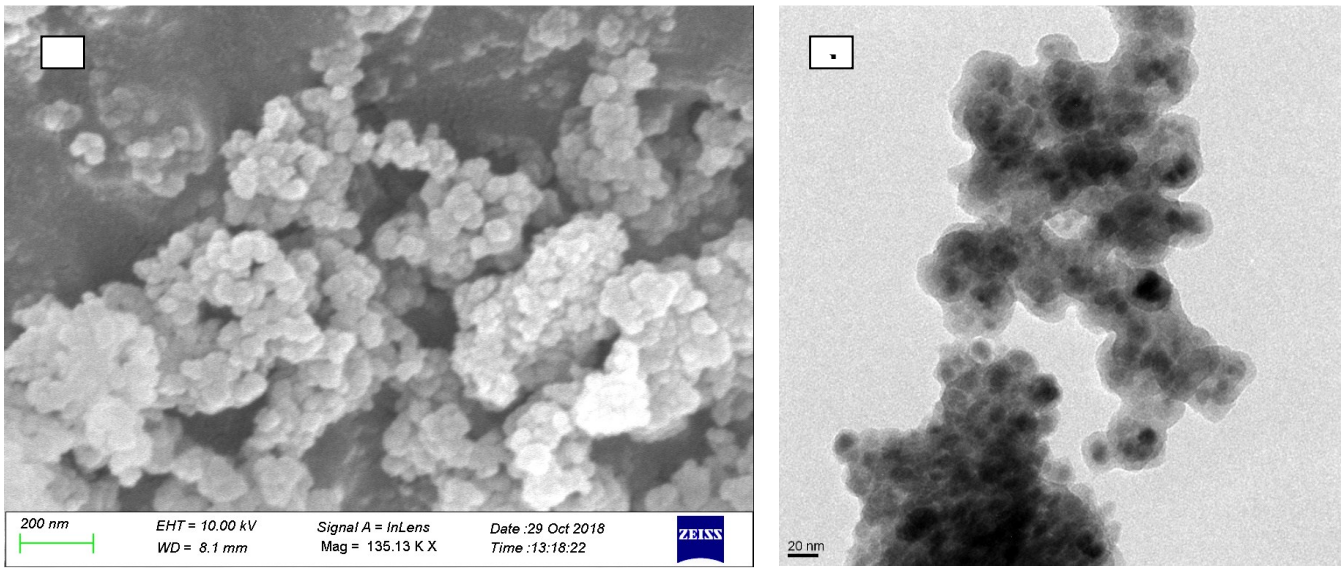


**Figure S11 a) SEM and b) TEM images of recovered catalyst after six runs.**

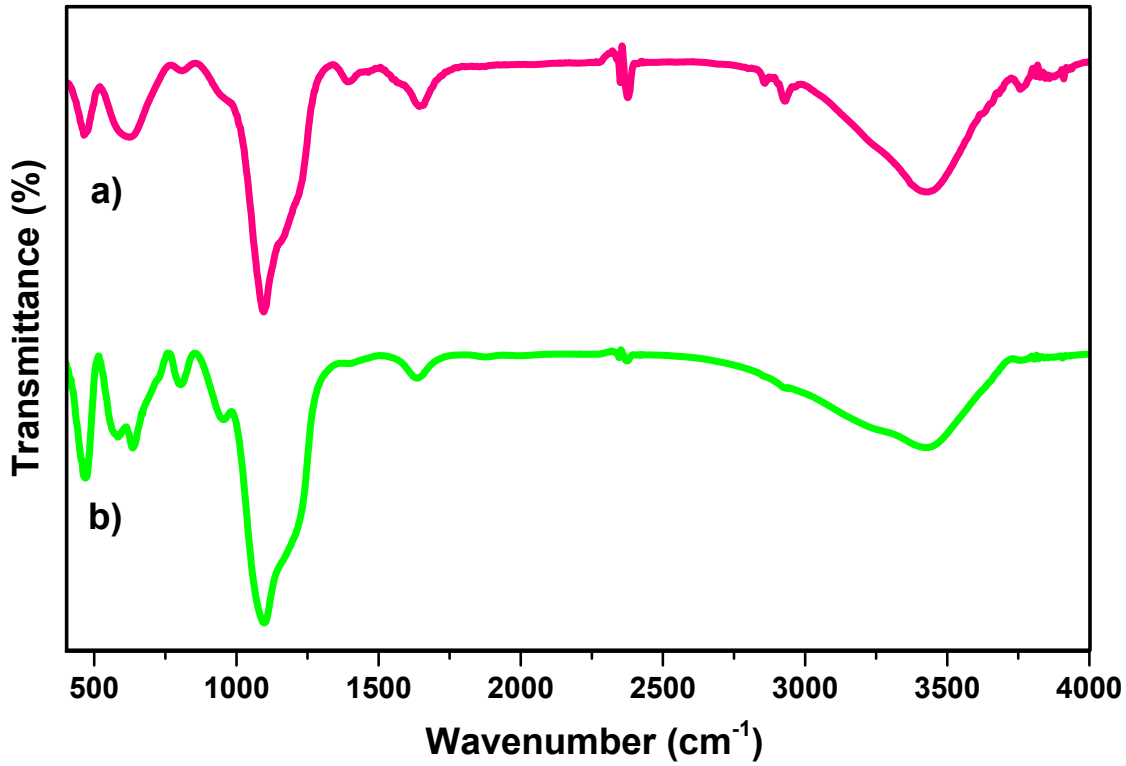


**Figure S12 FT-IR spectra of a) Fresh Ru@DAFO@ASMNPs and b) Recovered Ru@DAFO@ASMNPs catalyst after six runs.**

Furthermore, ICP-OES analysis was carried out to check the leaching of the metal which showed that there is negligible leaching and our catalyst is truly heterogeneous in nature. In addition, the morphology of Ru@DAFO@ASMNPs remains unchanged after six cycles which reveal the robust nature of the catalyst. The FE-SEM and TEM images reveal that no change in morphology occured after six successive runs (**Figure S11**). Moreover, the FT-IR spectrum of the recovered catalyst confirms the unaltered functional groups on the surface (**Figure S12**). VSM analysis discloses the significantly good magnetisation of the recovered catalyst (**Figure S7d**).

**Table S4 Comparison of the catalytic activities with the earlier reported heterogeneous photocatalysts for cross-dehydrogenative coupling.**

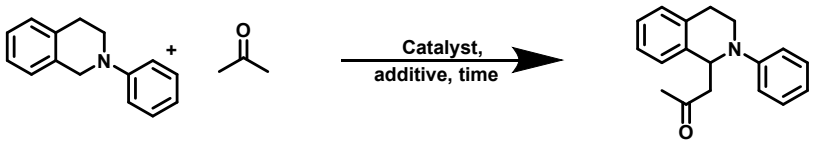


| Entry | Catalyst | Additive | Time (h) | % Yield[a] | Ref. |
|---|---|---|---|---|---|
| 1* | $[Ru(bpy)_3]PF_6$ | L-Proline | 24 | 95 | 9 |
| 2 | PDMS-RB | Pyrrolidine/TFA | 24 | 87 | 10 |
| 3 | AuNPore | $O_2$, 80 °C | 24 | 45 | 11 |
| 4 | CdS | L-Proline, $O_2$, High power LEDs | 24 | 100[b] | 12 |
| 5 | $TiO_2$ | L-Proline | 40 | 75 | 13 |
| 6 | UNLPF-12 | L-Proline | 48 | 98[c] | 14 |
| 7 | mpg-$C_3N_4$ | L-Proline, $O_2$, High power LEDs | 34 | 94 | 15 |
| 8 | COF-JLU5 | L-Proline, $O_2$, High power LEDs | 6 | 90 | 16 |
| **9** | **Ru@DAFO@ASMNPs** | **L-Proline, 10 W blue LEDs, air** | **24** | **83** | **Present work** |

[a] Isolated yield, [b]GC-MS yield, [c]NMR yield, *homogeneous catalyst.


**Figure S13 Photocatalytic reaction setup.**

## NMR DATA OF REACTANTS

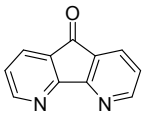

**4,5-diazafluoren-9-one** $^{1}$H NMR (400 MHz, $CDCl_3$) $\delta$ 8.73 (dd, $J$ = 5.0, 1.6 Hz, 2H), 7.92 (dd, $J$ = 7.6, 1.5 Hz, 2H), 7.29 (dd, $J$ = 7.5, 5.0 Hz, 2H); $^{13}$C NMR (100 MHz, $CDCl_3$) $\delta$ 189.6, 163.2, 155.3, 131.6, 129.4, 124.8.

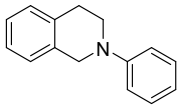

**2-phenyl-1,2,3,4-tetrahydroisoquinoline.** $^{1}$H NMR (400 MHz, $CDCl_3$) $\delta$ 7.40 (t, $J$ = 8.0 Hz, 2H), 7.27 (td, $J$ = 10.1, 4.7 Hz, 4H), 7.09 (d, $J$ = 7.8 Hz, 2H), 6.95 (t, $J$ = 7.3 Hz, 1H), 4.50 (s, 2H), 3.65 (t, $J$ = 5.9 Hz, 2H), 3.07 (t, $J$ = 5.9 Hz, 2H); $^{13}$C NMR (100 MHz, $CDCl_3$) $\delta$ 150.7, 135.1, 134.7, 129.1, 128.7, 126.8, 126.5, 126.2, 118.9, 115.4, 50.9, 46.7, 29.3.

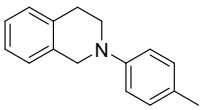

**2-(*p*-tolyl)-1,2,3,4-tetrahydroisoquinoline.** $^{1}$H NMR (400 MHz, $CDCl_3$) $\delta$ 7.19-7.06 (m, 6H), 6.93–6.90 (m, 2H), 4.34 (s, 2H), 3.49 (t, $J$ = 5.7 Hz, 2H), 2.96 (t, $J$ = 5.6 Hz, 2H), 2.27 (s, 3H); $^{13}$C NMR (100 MHz, $CDCl_3$) $\delta$ 147.0, 133.1, 128.1, 127.0, 124.9, 124.6, 124.3, 114.2, 49.8, 45.6, 27.5, 18.8.

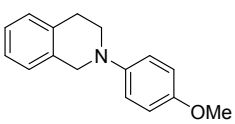

**2-(4-methoxyphenyl)-1,2,3,4-tetrahydroisoquinoline.** $^{1}$H NMR (400 MHz, $CDCl_3$) $\delta$ 7.05–6.97 (m, 4H), 6.86–6.82 (m, 2H), 6.75–6.70 (m, 2H), 4.14 (s, 2H), 3.61 (s, 3H), 3.28 (t, $J$ = 5.8 Hz, 2H), 2.83 (t, $J$ = 5.8 Hz, 2H); $^{13}$C NMR (100 MHz, $CDCl_3$) $\delta$ 170.73, 145.31, 134.62, 134.48, 128.32, 126.47, 126.16, 125.83, 117.94, 114.4, 60.2, 55.3, 29.1.

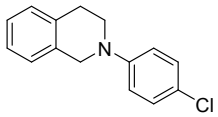

**2-(4-chlorophenyl)-1,2,3,4-tetrahydroisoquinoline.** $^1$H NMR (400 MHz, $CDCl_3$) $\delta$ 7.36–7.24 (m, 6H), 6.96 (d, $J$ = 9.2 Hz, 2H), 4.45 (s, 2H), 3.59 (t, $J$ = 5.7 Hz, 2H), 3.06 (t, $J$ = 5.7 Hz, 2H); $^{13}$C NMR (100 MHz, $CDCl_3$) $\delta$ 149.3, 134.9, 134.3, 129.27, 128.8, 126.8, 126.4, 123.4, 116.3, 50.8, 46.6, 29.3.

## NMR DATA OF PRODUCTS

## Mannich reaction: Substrate Scope

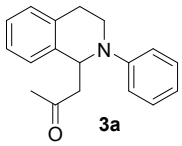

**3a**

**1-(2-phenyl-1,2,3,4-tetrahydroisoquinolin-1-yl)propan-2-one (3a).** $^1$H NMR (400 MHz, $CDCl_3$) $\delta$ 7.26 (t, $J$ = 8.0 Hz, 2H), 7.17–7.13 (m, 4H), 6.95 (d, $J$ = 8.2 Hz, 2H), 6.79 (t, $J$ = 7.3 Hz, 1H), 5.41 (t, $J$ = 6.4 Hz, 1H), 3.68–3.63 (m, 1H), 3.57–3.50 (m, 1H), 3.10–3.02 (m, 2H), 2.83 (dt, $J$ = 16.2, 3.5 Hz, 2H), 2.08 (s, 3H); $^{13}$C NMR (100 MHz, $CDCl_3$) $\delta$ 207.4, 150.0, 138.4, 134.5, 129.5, 128.8, 127.0, 126.9, 126.4, 118.4, 114.9, 54.9, 50.3, 42.1, 31.2, 27.3. HRMS (ESI) $[M+H]^+$ Calcd for $[C_{18}H_{20}NO]^+$ 266.1539, found 266.1562.

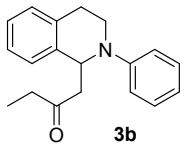

**3b**

**1-(2-phenyl-1,2,3,4-tetrahydroisoquinolin-1-yl)butan-2-one (3b).** $^1$H NMR (400 MHz, $CDCl_3$) $\delta$ 7.15–7.12 (m, 2H), 7.03 (s, 4H), 6.83 (d, $J$ = 8.0 Hz, 2H), 6.66 (t, $J$ = 7.1 Hz, 1H), 5.31 (t, $J$ = 6.3 Hz, 1H), 3.56–3.50 (m, 1H), 3.45–3.39 (m, 1H), 2.94 (td, $J$ = 15.3, 5.6 Hz, 2H), 2.75–2.64 (m, 2H), 2.28–2.09 (m, 2H), 0.87 (t, $J$ = 7.3 Hz, 3H); $^{13}$C NMR (100 MHz, $CDCl_3$) $\delta$ 210.0, 148.8, 138.3, 134.4, 129.3, 128.6, 126.8, 126.8, 126.2, 118.1, 114.6, 55.1, 48.9, 41.9, 37.3, 27.2, 7.5. HRMS (ESI) $[M+H]^+$ Calcd for $[C_{19}H_{22}NO]^+$ 280.1696, found 280.1659.

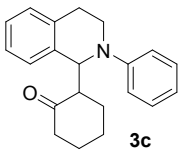

**3c**

**2-(2-phenyl-1,2,3,4-tetrahydroisoquinolin-1-yl)cyclohexan-1-one (3c)**. Isolated diastereomeric ratio = 5:1; $^1$H NMR (400 MHz, $CDCl_3$) $\delta$ 7.34–7.09 (m, mixture of isomers, 12 H), 6.90 (d, $J$ = 8.0 Hz, 2H, major isomer), 6.81 (d, $J$ = 8.2 Hz, 2H, minor isomer), 6.76 (t, $J$ = 7.2 Hz, 1H, major isomer), 6.68 (t, $J$ = 7.3 Hz, 1H, minor isomer), 5.66 (d, $J$ = 8.7 Hz, 1H, minor isomer), 5.60 (d, $J$ = 4.7 Hz, 1H, major isomer), 4.15-4.08 (m, 2H, minor isomer), 3.75-3.68 (m, 1H, major isomer), 3.61–3.52 (m, 1H, major isomer), 3.06–2.81 (m, 4H, mixture of isomers), 2.76–2.69 (m, 1H, minor isomer), 2.50–2.43 (m, 2H, mixture of isomers), 2.33–1.17 (m, 2H, mixture of isomers), 1.95–1.89 (m, 4H, mixture of isomers), 1.75-1.57 (m, 6H, mixture of isomer), 1.48-1.38 (m, 1H, major isomer), 1.29-1.24 (m, 2H, mixture of isomer); $^{13}$C NMR (100 MHz, $CDCl_3$) Major isomer: $\delta$ 212.07, 149.30, 136.03, 135.13, 129.41, 128.75, 128.03, 126.75, 125.86, 118.22, 114.98, 56.58, 54.87, 42.66, 41.45, 30.24, 27.42, 27.30, 23.85; Minor isomer: $\delta$ 140.42, 134.65, 129.32, 127.90, 127.30, 126.40, 116.43, 112.34, 59.40, 54.09, 43.62, 43.28, 32.89, 28.77, 25.77. HRMS (ESI) $[M+H]^+$ Calcd for $[C_{21}H_{24}NO]^+$ 306.1852, found 306.1833.

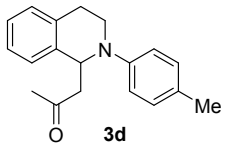

**3d**

**1-(2-(p-tolyl)-1,2,3,4-tetrahydroisoquinolin-1-yl)propan-2-one (3d).** $^1$H NMR (400 MHz, $CDCl_3$) $\delta$ 7.18–7.12 (m, 4H), 7.07 (d, $J$ = 7.8 Hz, 2H), 6.88 (d, $J$ = 10.1 Hz, 2H), 5.36 (t, $J$ = 6.4 Hz, 1H), 3.67–3.61 (m, 1H), 3.55–3.47 (m, 1H), 3.09–3.01 (m, 2H), 2.84–2.76 (m, 2H), 2.27 (s, 3H), 2.08 (s, 3H);

$^{13}$C NMR (100 MHz, $CDCl_3$) $\delta$ 206.9, 146.4, 137.8, 133.9, 129.3, 128.3, 127.4, 126.3, 126.2, 125.7, 115.2, 54.7, 49.5, 41.7, 30.5, 26.5, 19.8. HRMS (ESI) $[M+H]^+$ Calcd for $[C_{19}H_{22}NO]^+$ 280.1696, found 280.1699.

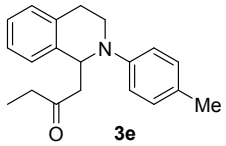


**3e**

**1-(2-(p-tolyl)-1,2,3,4-tetrahydroisoquinolin-1-yl)butan-2-one (3e).** $^1$H NMR (400 MHz, $CDCl_3$) $\delta$ 7.15–7.09 (m, 4H), 7.04 (d, $J$ = 8.4 Hz, 2H), 6.85 (d, $J$ = 8.7 Hz, 2H), 5.35 (t, $J$ = 6.5 Hz, 1H), 3.65–3.58 (m, 1H), 3.52–3.45 (m, 1H), 3.08–2.97 (m, 2H), 2.81–2.71 (m, 2H), 2.41–2.22 (m, 5H), 0.96 (t, $J$ = 7.3 Hz, 3H); $^{13}$C NMR (100 MHz, $CDCl_3$) $\delta$210.2, 147.0, 138.5, 134.5, 129.9, 128.8, 127.9, 127.0, 126.8, 126.2, 115.5, 55.5, 48.9, 42.1, 37.3, 27.1, 20.4, 7.6. HRMS (ESI) $[M+H]^+$ Calcd for $[C_{20}H_{24}NO]^+$ 294.1852, found 294.1853.

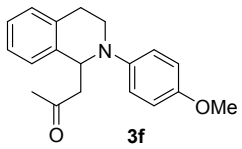


**3f**

**1-(2-(4-methoxyphenyl)-1,2,3,4-tetrahydroisoquinolin-1-yl)propan-2-one (3f).** $^1$H NMR (400 MHz, $CDCl_3$) $\delta$ 7.16–7.09 (m, 4H), 6.90 (d, $J$ = 9.2 Hz, 2H), 6.80 (d, $J$ = 9.1 Hz, 2H), 5.23 (t, $J$ = 6.4 Hz, 1H), 3.74 (s, 3H), 3.55 (ddd, J = 13.0, 5.7, 3.7 Hz, 1H), 3.48–3.41 (m, 1H), 3.03–2.95 (m, 2H), 2.78–2.69 (m, 2H), 2.05 (s, 3H); $^{13}$C NMR (100 MHz, $CDCl_3$) $\delta$ 207.5, 153.4, 143.8, 138.4, 134.4, 129.0, 126.9, 126.7, 126.3, 118.5, 114.7, 56.1, 55.7, 50.1, 43.0, 31.0, 26.8. HRMS (ESI) $[M+H]^+$ Calcd for $[C_{19}H_{22}NO_2]^+$ 296.1645, found 296.1643.

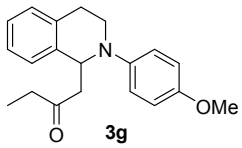


**3g**

**1-(2-(4-methoxyphenyl)-1,2,3,4-tetrahydroisoquinolin-1-yl)butan-2-one (3g)**. $^1$H NMR (400 MHz, $CDCl_3$) $\delta$ 7.16–7.10 (m, 4H), 6.94–6.90 (m, 2H), 6.84–6.80 (m, 2H), 5.28 (t, $J$ = 6.4 Hz, 1H), 3.74 (s, 3H), 3.58–3.53 (m, 1H), 3.49–3.42 (m, 1H), 3.06–2.96 (m, 2H), 2.78–2.70 (m, 2H), 2.39–2.20 (m, 2H), 0.97 (t, $J$ = 7.3 Hz, 3H); $^{13}$C NMR (100 MHz, $CDCl_3$) $\delta$ 210.2, 153.3, 143.8, 138.5, 134.4, 129.0, 126.9, 126.7, 126.2, 118.2, 114.8, 56.3, 55.7, 48.8, 42.8, 37.2, 27.0, 7.6. HRMS (ESI) $[M+H]^+$ Calcd for $[C_{20}H_{24}NO_2]^+$ 310.1802, found 310.1834.

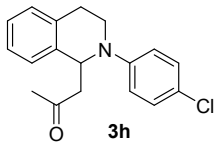


**3h**

**1-(2-(4-chlorophenyl)-1,2,3,4-tetrahydroisoquinolin-1-yl)propan-2-one (3h).** $^1$H NMR (400 MHz, $CDCl_3$) $\delta$ 7.18–7.12 (m, 6H), 6.85 (d, $J$ = 8.0 Hz, 2H), 5.34 (t, $J$ = 6.3 Hz, 1H), 3.62–3.56 (m, 1H), 3.54–3.47 (m, 1H), 3.07–2.99 (m, 2H), 2.85–2.79 (m, 2H), 2.08 (s, 3H); $^{13}$C NMR (100 MHz, $CDCl_3$) $\delta$ 207.2, 147.6, 138.0, 134.3, 129.4, 129.2, 128.8, 127.1, 126.9, 126.5, 123.1, 115.9, 54.9, 50.2, 42.3, 31.2, 27.1. HRMS (ESI) $[M+H]^+$ Calcd for $[C_{18}H_{19}ClNO]^+$ 300.1150, found 300.1119.

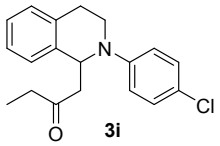


**3i**

**1-(2-(4-chlorophenyl)-1,2,3,4-tetrahydroisoquinolin-1-yl)butan-2-one (3i).** $^1$H NMR (400 MHz, $CDCl_3$) $\delta$ 7.19–7.11 (m, 6H), 6.86 (d, $J$ = 9.1 Hz, 2H), 5.36 (t, $J$ = 6.4 Hz, 1H), 3.62–3.48 (m, 2H), 3.08–2.98 (m, 2H), 2.86–2.75 (m, 2H), 2.41–2.21 (m, 2H), 0.99 (t, $J$ = 7.3 Hz, 3H); $^{13}$C NMR (100 MHz, $CDCl_3$) $\delta$ 209.9, 147.5, 138.1, 134.3, 129.2, 128.8, 127.0, 126.9, 126.5, 122.9, 115.7, 55.2, 49.0, 42.2, 37.4, 27.2, 7.6. HRMS (ESI) $[M+H]^+$ Calcd for $[C_{19}H_{21}ClNO]^+$ 314.1306, found 314.1311.

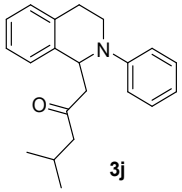


**3j**

**4-Methyl-1-(2-phenyl-1,2,3,4-tetrahydroisoquinolin-1-yl)pentan-2-one (3j).** $^1$H NMR (400 MHz, $CDCl_3$) $\delta$ 7.33-7.22 (m, 2H), 7.20-7.12 (m, 4H), 6.96 (d, $J$ = 7.8 Hz, 2H), 6.78 (t, $J$ = 7.2 Hz, 1H), 5.44 (t, $J$ = 6.3 Hz, 1H), 3.67-3.60 (m, 1H), 3.58-3.50 (m, 1H), 3.11-3.01 (m, 2H), 2.87-2.74 (m, 2H), 2.24-2.01

(m, 3H), 0.85 (d, *J* = 3.3 Hz, 3H), 0.83 (d, *J* = 3.3 Hz, 3H); $^{13}$C NMR (100 MHz, $CDCl_3$) $\delta$ 209.3, 148.9, 138.6, 134.5, 129.4, 128.7, 127.0, 126.8, 126.3, 118.2, 114.6, 54.8, 53.1, 49.8, 42.1, 27.4, 24.5, 22.6.

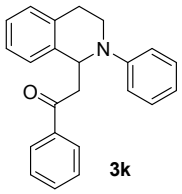

**3k**

**1-Phenyl-2-(2-phenyl-1,2,3,4-tetrahydroisoquinolin-1-yl)ethan-1-one (3k).** $^1$H NMR (400 MHz, $CDCl_3$) $\delta$ 7.84 (dd, *J* = 8.3, 1.3 Hz, 2H), 7.54-7.49 (m, 1H), 7.40 (t, *J* = 7.7 Hz, 2H), 7.23 (dd, J = 8.9, 7.5 Hz, 3H), 7.16-7.08 (m, 3H), 6.96 (d, *J* = 8.1 Hz, 2H), 6.74 (t, *J* = 7.2 Hz, 1H), 5.67-5.64 (m, 1H), 3.69-3.54 (m, 3H), 3.39 (dd, *J* = 16.6, 7.4 Hz, 1H), 3.15-3.07 (m, 1H), 2.92 (dt, *J* = 16.0, 5.2 Hz, 1H); $^{13}$C NMR (100 MHz, $CDCl_3$) $\delta$198.7, 148.8, 138.6, 134.6, 133.2, 129.4, 128.6, 128.2, 127.2, 126.9, 126.3, 118.0, 114.4, 55.1, 45.4, 42.2, 27.6. HRMS (ESI) $[M+H]^+$ Calcd for $[C_{23}H_{22}NO]^+$ 328.1696, found 328.1698.

## Nitro-Mannich reaction: Substrate Scope

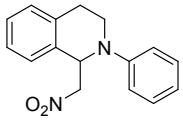

**5a**

**1-(nitromethyl)-2-phenyl-1,2,3,4-tetrahydroisoquinoline (5a)**. $^1$H NMR (400 MHz, $CDCl_3$) $\delta$ 7.33–7.18 (m, 5H), 7.14 (d, *J* = 7.0 Hz, 1H), 7.00 (d, *J* = 8.2 Hz, 2H), 6.87 (t, *J* = 7.3 Hz, 1H), 5.57 (t, *J* = 7.2 Hz, 1H), 4.87 (dd, *J* = 11.8, 7.8 Hz, 1H), 4.57 (dd, *J* = 12.0, 6.6 Hz, 1H), 3.72–3.56 (m, 2H), 3.15–3.03 (m, 1H), 2.85–2.75 (dt, *J* = 16.4, 4.9 Hz, 1H); $^{13}$C NMR (100 MHz, $CDCl_3$) $\delta$ 148.6, 135.4, 133.0, 129.6, 129.3, 128.2, 127.1, 126.8, 119.5, 115.2, 78.9, 58.3, 42.1, 26.5. HRMS (ESI) $[M+H]^+$ Calcd for $[C_{16}H_{17}N_2O_2]^+$ 269.1285, found 269.1291.

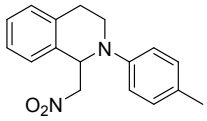

**5b**

**1-(nitromethyl)-2-(*p*-tolyl)-1,2,3,4-tetrahydroisoquinoline (5b).** $^1$H NMR (400 MHz, $CDCl_3$) $\delta$ 7.29–7.14 (m, 4H), 7.10 (d, *J* = 8.2 Hz, 2H), 6.92 (d, *J* = 8.5 Hz, 2H), 5.52 (t, *J* = 7.2 Hz, 1H), 4.85 (dd, *J* = 11.9, 8.2 Hz, 1H), 4.56 (dd, *J* = 12.0, 6.3 Hz, 1H), 3.52–3.69 (m, 2H), 3.04–3.12 (m, 1H), 2.76 (dt, *J* = 16.4, 4.5 Hz, 1H), 2.29 (s, 3H); $^{13}$C NMR (100 MHz, $CDCl_3$) $\delta$ 146.5, 135.5, 133.1, 130.1, 129.4, 129.2, 128.1, 127.1, 126.7, 116.0, 78.9, 58.5, 42.4, 26.3, 20.5. HRMS (ESI) $[M+H]^+$ Calcd for $[C_{17}H_{19}N_2O_2]^+$ 283.1441, found 283.1406.

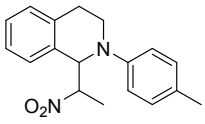

**5c**

**1-(1-nitroethyl)-2-(p-tolyl)-1,2,3,4-tetrahydroisoquinoline (5c).** Isolated diastereomeric ratio = 3:2; $^1$H NMR (400 MHz, $CDCl_3$) $\delta$ 7.30–7.06 (m, 12H, mixture of isomers), 6.97-6.94 (m, 4H, mixture of isomers), 5.26-5.21 (m, 2H, mixture of isomers), 5.11–5.04 (m, 1H, major isomer), 4.97–4.90 (m, 1H, minor isomer), 3.88–3.81 (m, 2H, minor isomer), 3.62–3.52(m, 2H, major isomer), 3.10–3.03 (m, 2H, minor isomer), 2.93–2.83 (m, 2H, major isomer), 2.32 (s, 3H, minor isomer), 2.30 (s, 3H, major isomer), 1.73 (d, *J* = 6.9 Hz, 3H, minor isomer), 1.57 (d, *J* = 6.9 Hz, 3H, major isomer); $^{13}$C NMR (100 MHz, $CDCl_3$); major isomers : $\delta$ 146.9, 135.9, 132.2, 130.0, 129.0, 128.5, 128.3, 126.2, 116.2, 85.7, 63.1, 42.9, 26.3, 20.5, 16.6; minor isomers : $\delta$ 147.3, 135.1, 134.0, 130.1, 129.3, 129.0, 127.4, 126.6, 115.3, 89.1, 61.6, 44.0, 26.7, 20.4, 17.5. HRMS (ESI) $[M+H]^+$ Calcd for $[C_{18}H_{21}N_2O_2]^+$ 297.1598, found 297.1594.

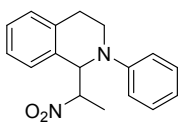

**5d**

**1-(1-nitroethyl)-2-phenyl-1,2,3,4-tetrahydroisoquinoline (5d).** Isolated diastereomeric ratio = 2:1; $^1$H NMR (400 MHz, $CDCl_3$) $\delta$ 7.30–7.10 (m, 12 H, mixture of isomers), 7.02–7.00 (m, 4H, mixture of isomers), 6.84–6.80 (m, 2H, mixture of isomers), 5.26–5.22 (m, 2H, mixture of isomers), 5.08–5.00 (m, 1H, major isomers), 4.94–4.85 (m, 1H, minor isomers), 3.87–3.80 (m, 2H, minor isomers), 3.62–3.52 (m, 2H, major isomers), 3.09–2.83 (m, 4H, mixture of isomers), 1.70 (d, *J* = 6.9 Hz, 3H, minor isomers), 1.54 (d, *J* = 6.7 Hz, 3H, major isomers); $^{13}$C NMR (100 MHz, $CDCl_3$);

major isomer: $\delta$ 148.9, 135.7, 132.10, 126.2, 119.42, 115.51, 85.5, 62.8, 42.8, 26.5, 16.3; Minor isomer: $\delta$ 149.2, 134.9, 133.9, 129.4, 128.80, 126.7, 118.88, 114.57, 89.1, 61.2, 43.7, 26.8, 17.52. HRMS (ESI) $[M+H]^+$ Calcd for $[C_{17}H_{19}N_2O_2]^+$ 283.1441, found 283.1426.

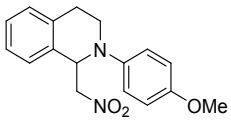


**5e**

**2-(4-Methoxyphenyl)-1-(nitromethyl)-1,2,3,4-tetrahydroisoquinoline (5e).** $^1$H NMR (400 MHz, $CDCl_3$) $\delta$ 7.27-7.21 (m, 2H), 7.18-7.13 (m, 2H), 6.93-6.90 (m, 2H), 6.84-6.81 (m, 2H), 5.39 (dd, $J$ = 8.6, 5.8 Hz, 1H), 4.83 (dd, $J$ = 12.0, 8.7 Hz, 1H), 4.57 (q, $J$ = 5.9 Hz, 1H), 3.75 (s, 3H), 3.59-3.53 (m, 2H), 3.06-2.98 (m, 1H), 2.70 (dt, $J$ = 16.5, 3.8 Hz, 1H); $^{13}$C NMR (100 MHz, $CDCl_3$) $\delta$ 154.0, 143.1, 135.5, 132.9, 129.6, 128.0, 127.0, 126.7, 119.0, 114.8, 79.0, 59.0, 55.7, 43.2, 25.9. HRMS (ESI) $[M+H]^+$ Calcd for $[C_{17}H_{19}N_2O_3]^+$ 299.1390, found 299.1391.

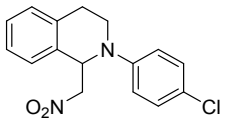


**5f**

**2-(4-chlorophenyl)-1-(nitromethyl)-1,2,3,4-tetrahydroisoquinoline (5f).** $^1$H NMR (400 MHz, $CDCl_3$) $\delta$ 7.27–7.17 (m, 5H), 7.13 (d, $J$ = 7.3 Hz, 1H), 6.86–6.90 (m, 2H), 5.46–5.49 (m, 1H), 4.84 (dd, $J$ = 12.0, 8.1 Hz, 1H), 4.56 (dd, $J$ = 12.0, 6.3 Hz, 1H), 3.59–3.63 (m, 2H), 3.02–3.09 (m, 1H), 2.77 (dt, $J$ = 16.4, 4.8 Hz, 1H); $^{13}$C NMR (100 MHz, $CDCl_3$) $\delta$ 147.2, 135.2, 132.6, 129.4, 128.4, 127.1, 126.9, 124.5, 116.6, 78.8, 58.3, 42.3, 26.2. HRMS (ESI) $[M+H]^+$ Calcd for $[C_{16}H_{16}ClN_2O_2]^+$ 303.0895, found 303.0879.

## NMR Spectra

### $^{1}$H NMR

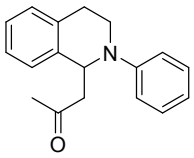

**1-(2-phenyl-1,2,3,4-tetrahydroisoquinolin-1-yl)propan-2-one (3a)**

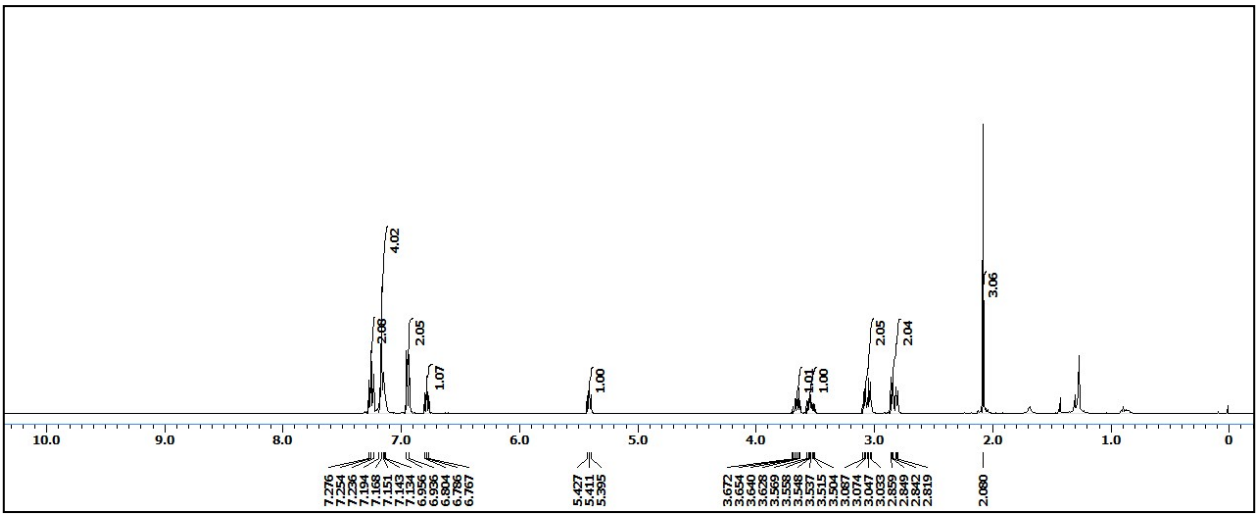


### $^{13}$C NMR

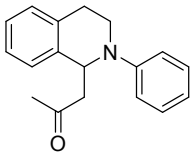

**1-(2-phenyl-1,2,3,4-tetrahydroisoquinolin-1-yl)propan-2-one (3a)**

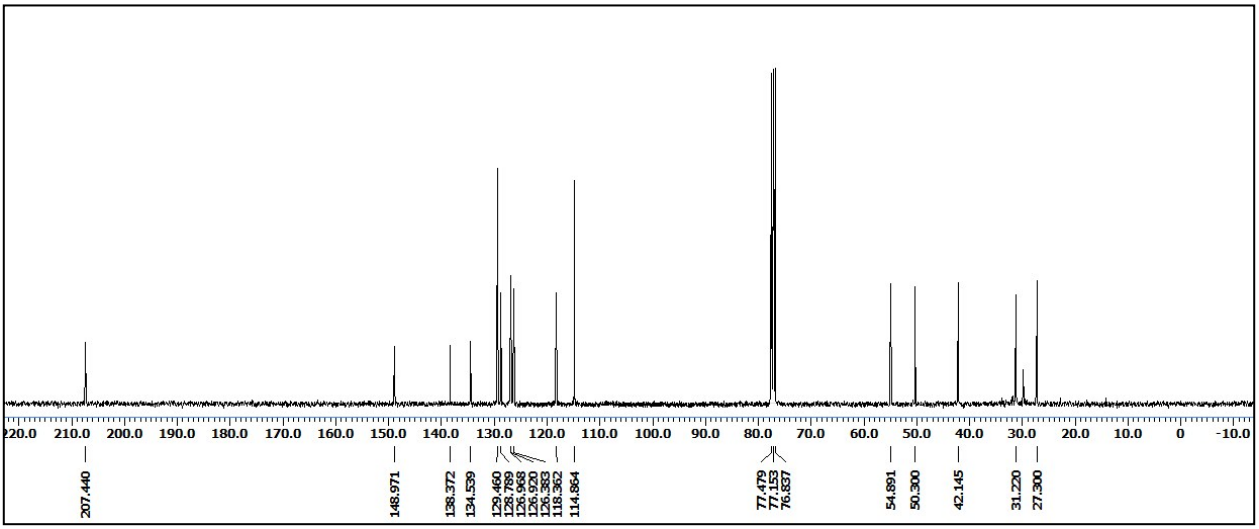

**$^{1}$H NMR**

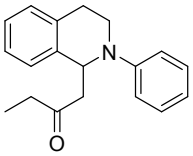

**1-(2-phenyl-1,2,3,4-tetrahydroisoquinolin-1-yl)butan-2-one (3b)**

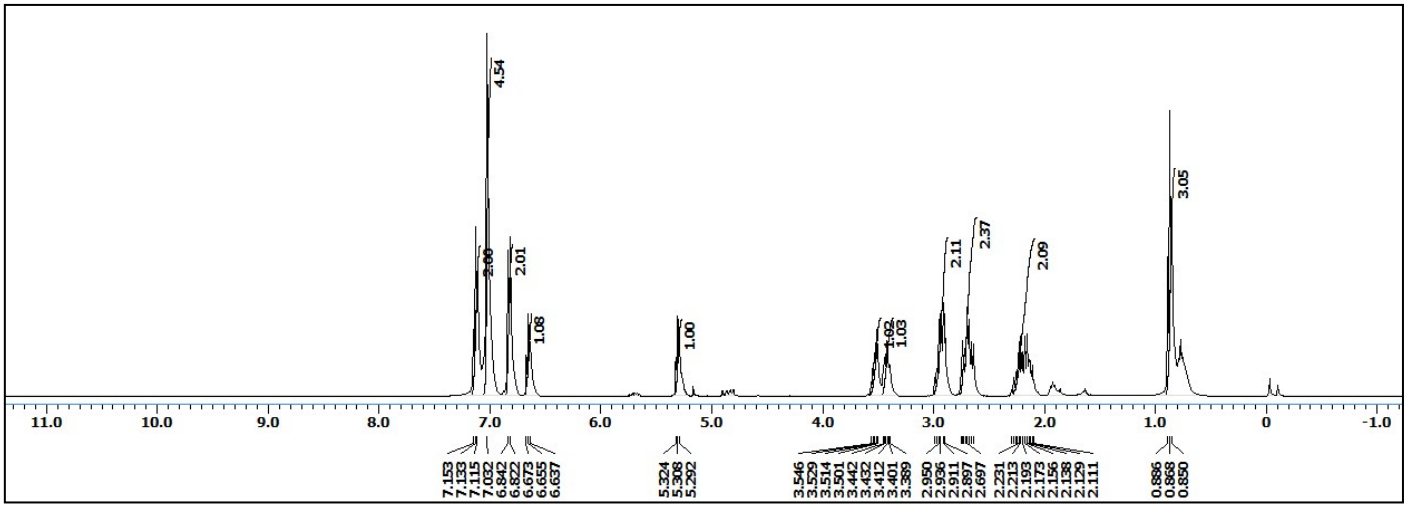


**$^{13}$C NMR**

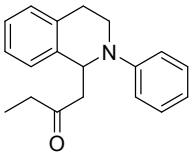

**1-(2-phenyl-1,2,3,4-tetrahydroisoquinolin-1-yl)butan-2-one (3b)**

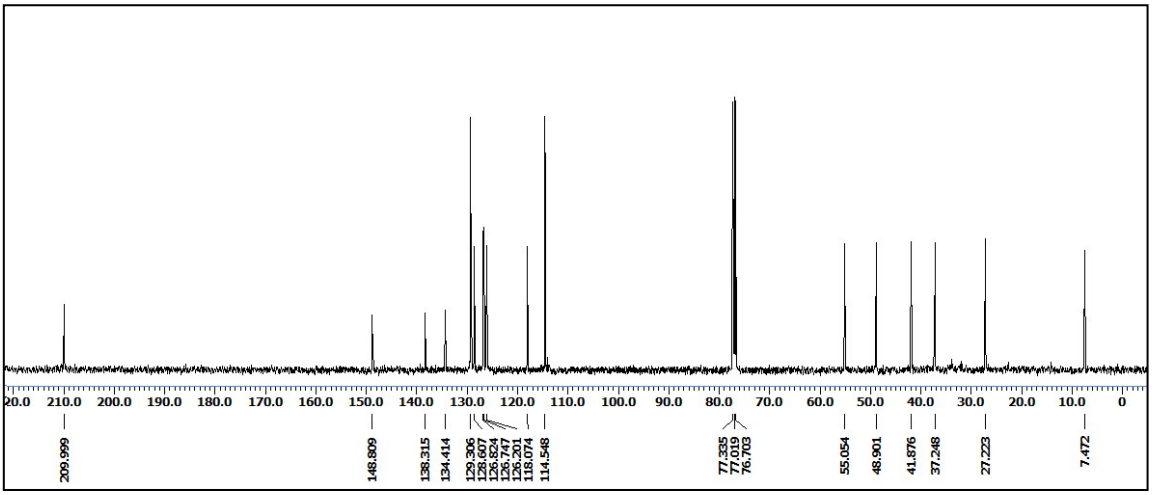

**$^{1}$H NMR**

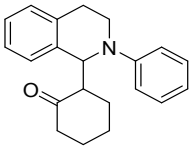

**2-(2-phenyl-1,2,3,4-tetrahydroisoquinolin-1-yl)cyclohexan-1-one (3c)**

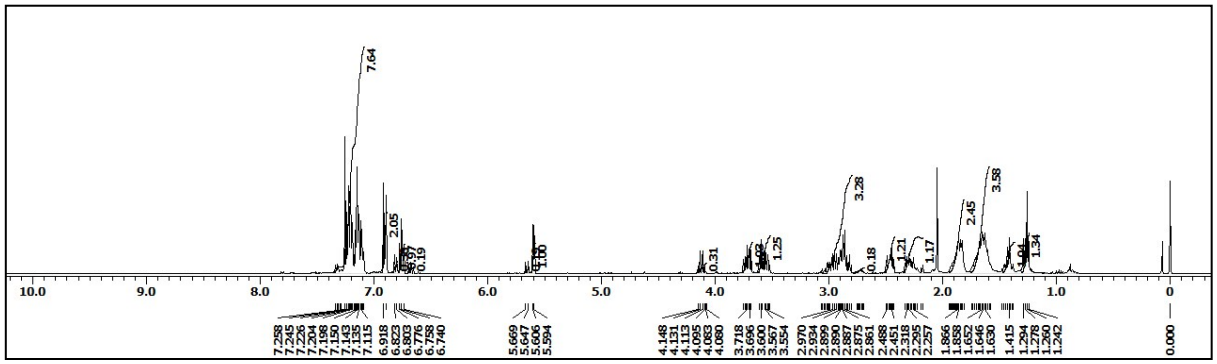

**$^{13}$C NMR**

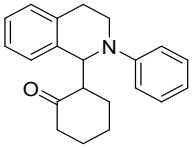

**2-(2-phenyl-1,2,3,4-tetrahydroisoquinolin-1-yl)cyclohexan-1-one (3c)**

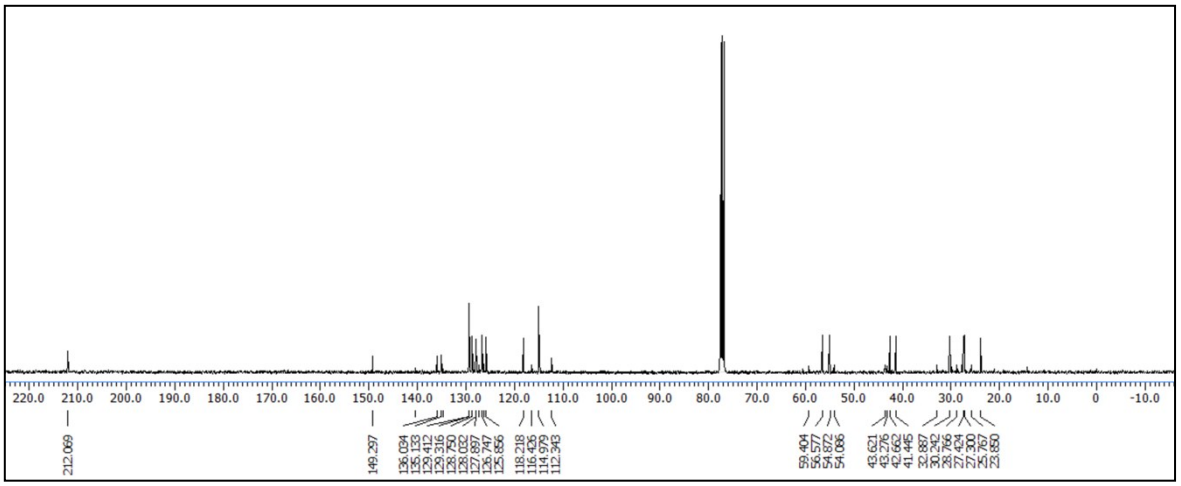

**$^{1}$H NMR**

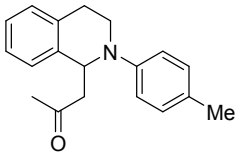


**1-(2-(p-tolyl)-1,2,3,4-tetrahydroisoquinolin-1-yl)propan-2-one (3d)**

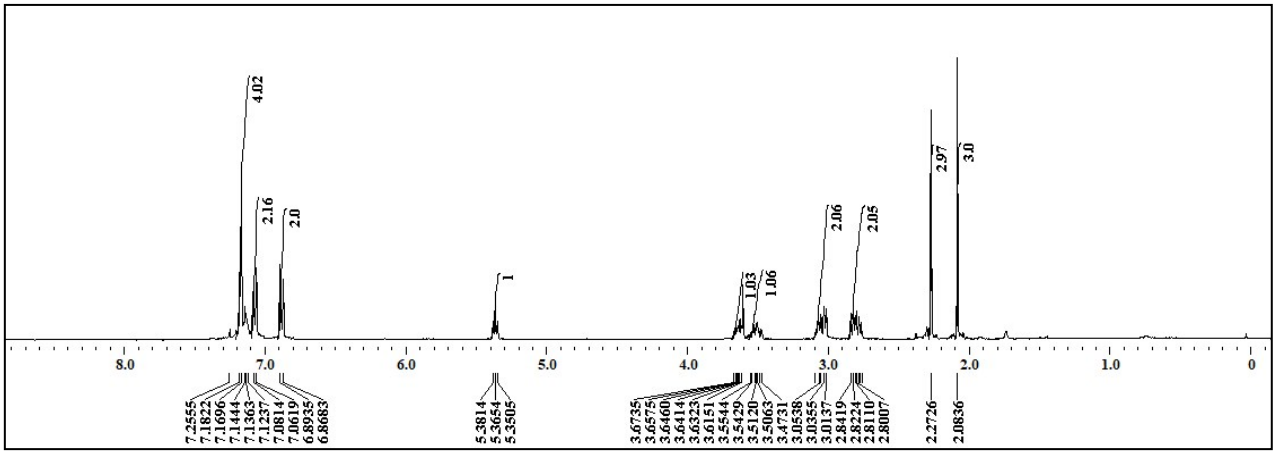


**$^{13}$C NMR**

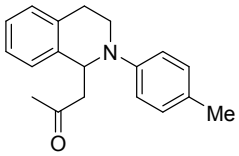


**1-(2-(p-tolyl)-1,2,3,4-tetrahydroisoquinolin-1-yl)propan-2-one (3d)**

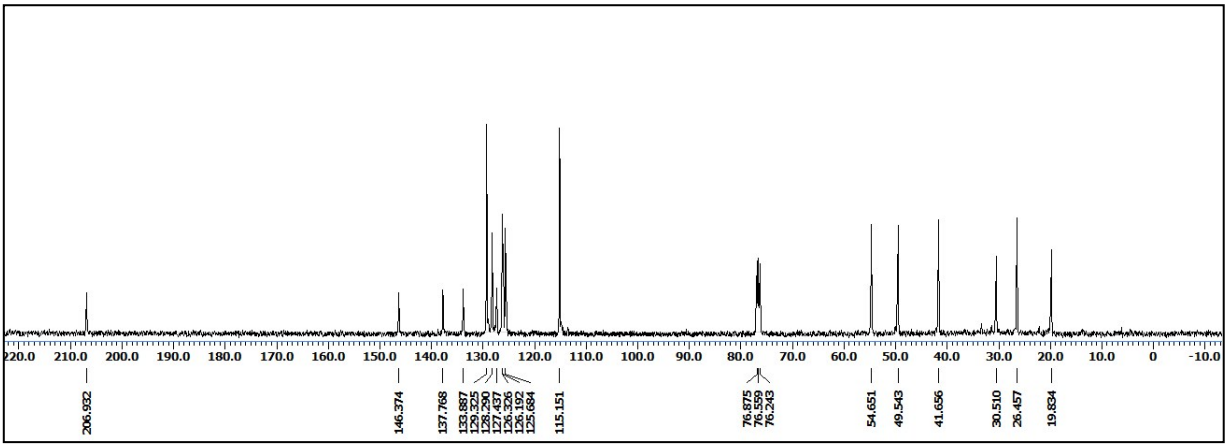

**$^{1}$H NMR**

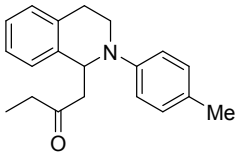


**1-(2-(p-tolyl)-1,2,3,4-tetrahydroisoquinolin-1-yl)butan-2-one (3e)**

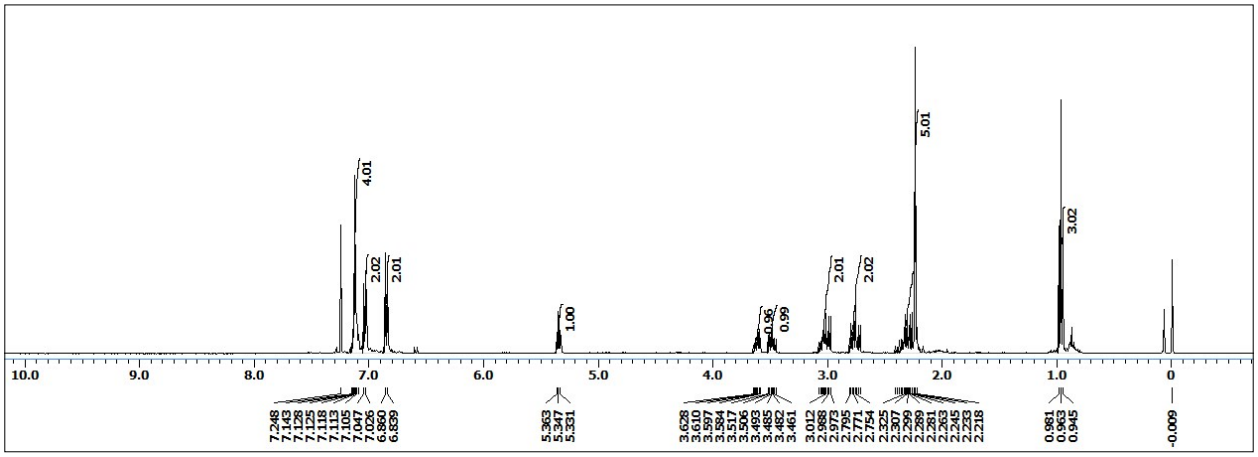


**$^{13}$C NMR**

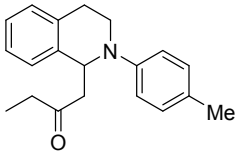


**1-(2-(p-tolyl)-1,2,3,4-tetrahydroisoquinolin-1-yl)butan-2-one (3e)**

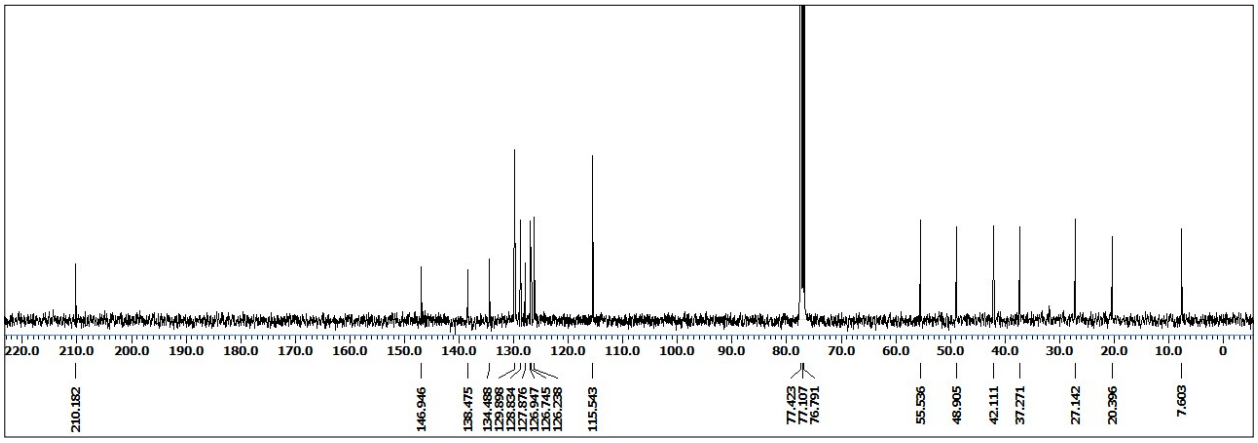

**$^{1}$H NMR**

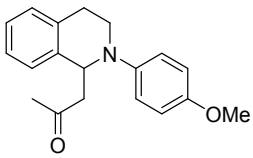


**1-(2-(4-methoxyphenyl)-1,2,3,4-tetrahydroisoquinolin-1-yl)propan-2-one (3f)**

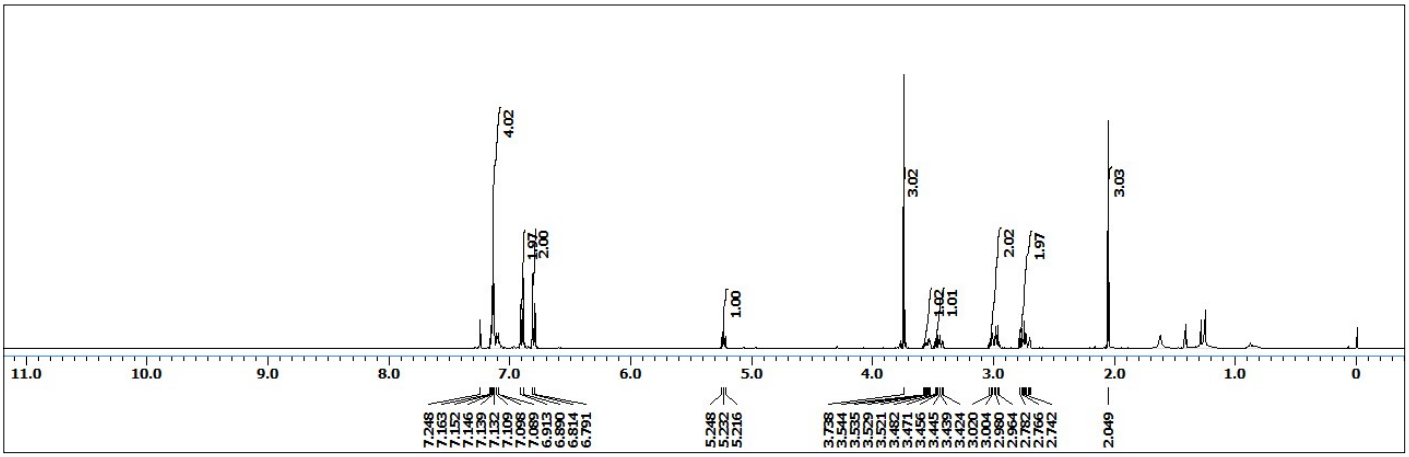


**$^{13}$C NMR**

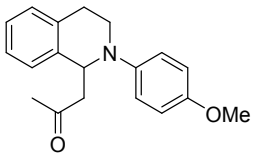


**1-(2-(4-methoxyphenyl)-1,2,3,4-tetrahydroisoquinolin-1-yl)propan-2-one (3f)**

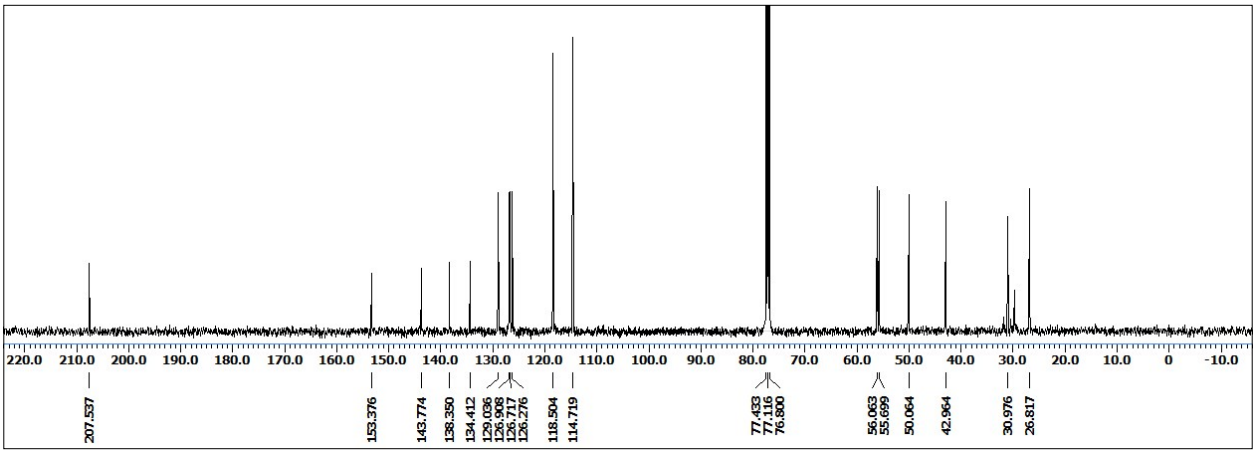

**$^{1}$H NMR**

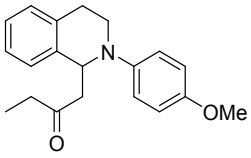


**1-(2-(4-methoxyphenyl)-1,2,3,4-tetrahydroisoquinolin-1-yl)butan-2-one (3g)**

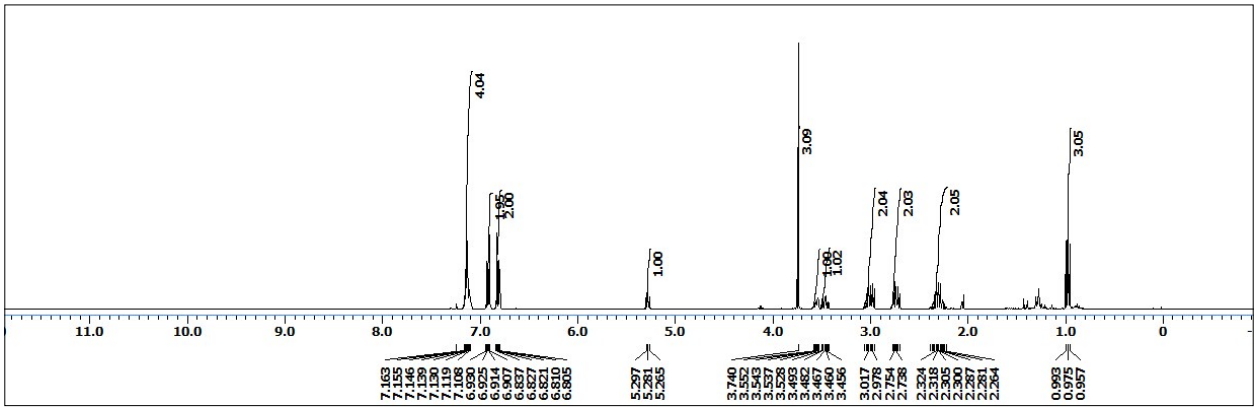


**$^{13}$C NMR**

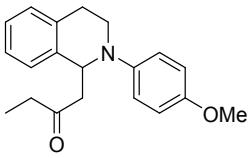


**1-(2-(4-methoxyphenyl)-1,2,3,4-tetrahydroisoquinolin-1-yl)butan-2-one (3g)**

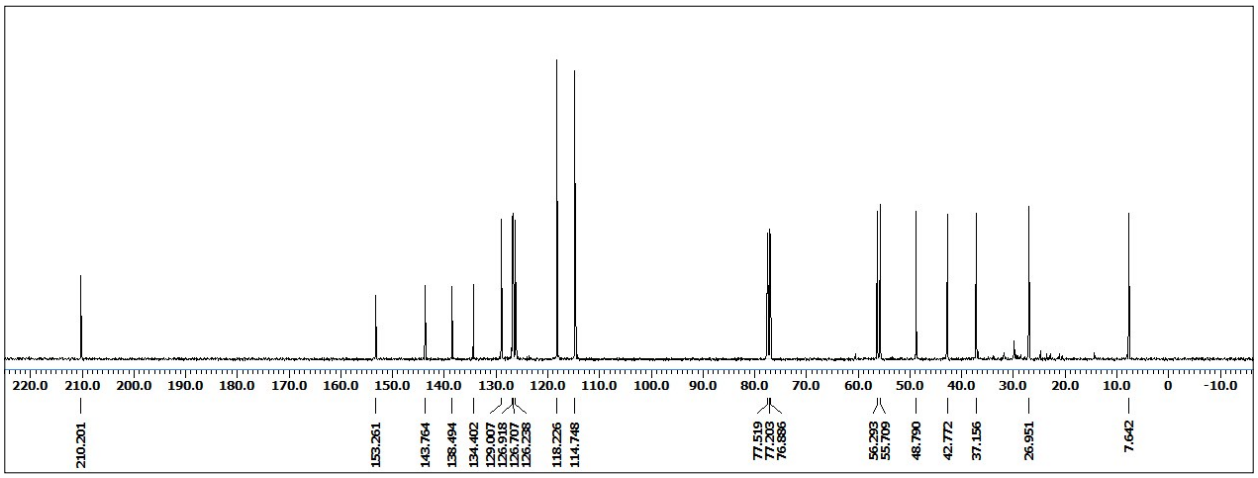

**$^{1}$H NMR**

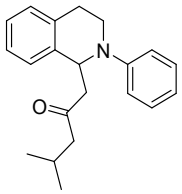

**4-Methyl-1-(2-phenyl-1,2,3,4-tetrahydroisoquinolin-1-yl)pentan-2-one (3h)**

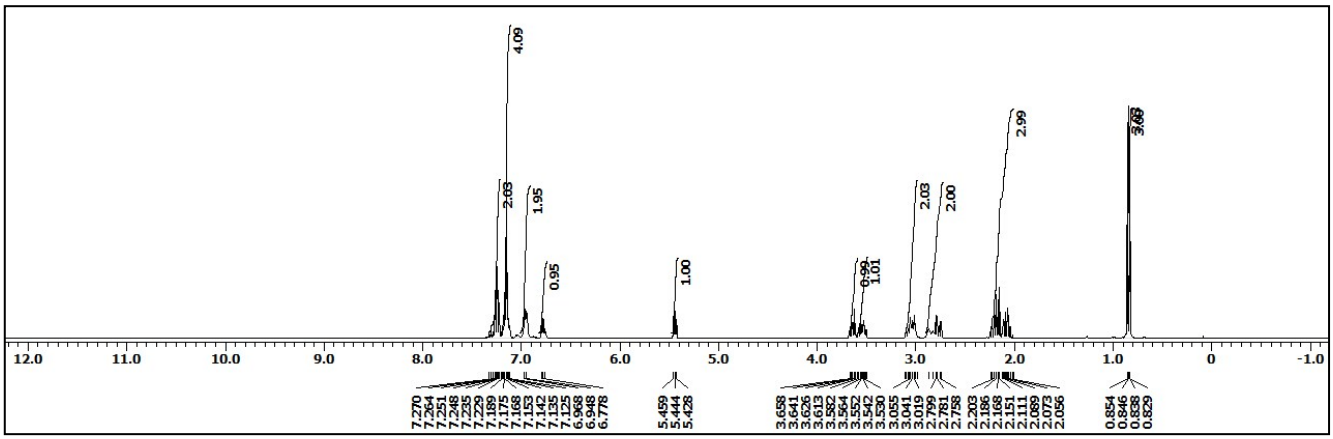

**$^{13}$C NMR**

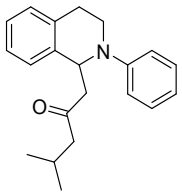

**4-Methyl-1-(2-phenyl-1,2,3,4-tetrahydroisoquinolin-1-yl)pentan-2-one (3h)**

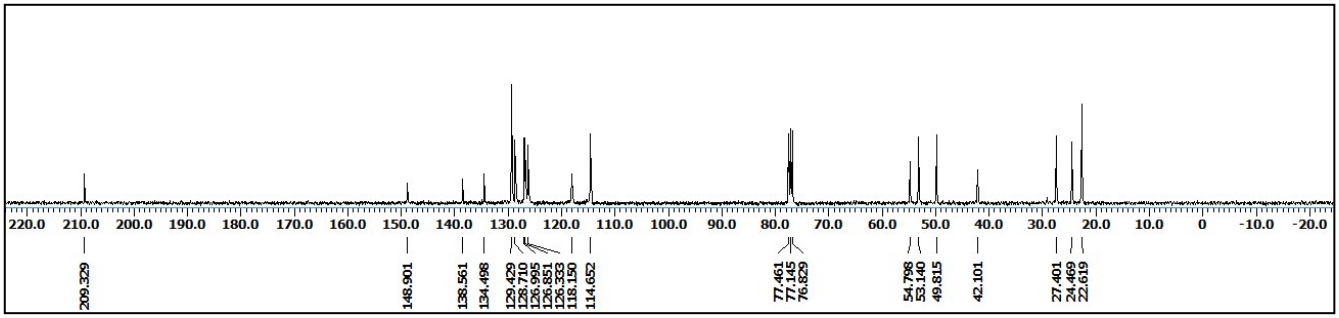

**$^{1}$H NMR**

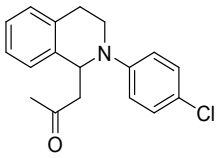


**1-(2-(4-chlorophenyl)-1,2,3,4-tetrahydroisoquinolin-1-yl)propan-2-one (3i)**

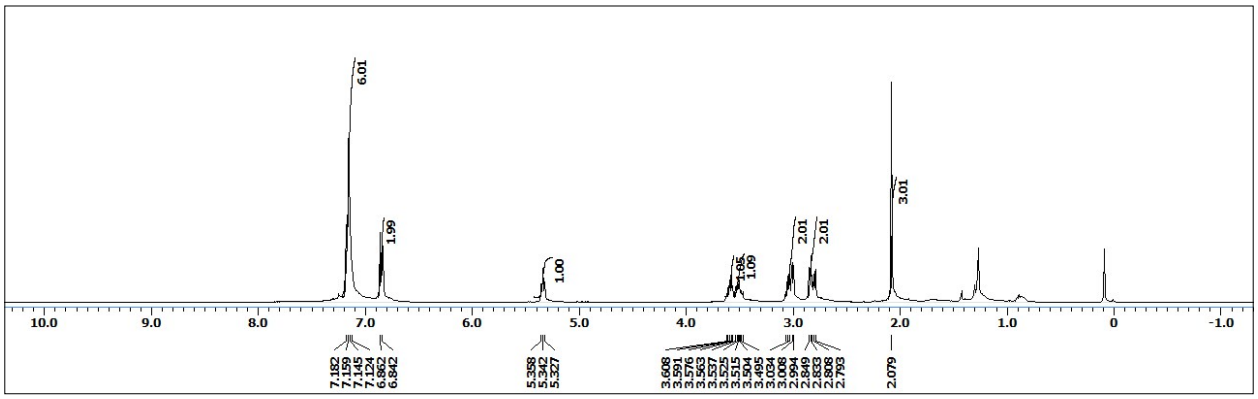


**$^{13}$C NMR**

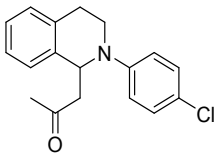


**1-(2-(4-chlorophenyl)-1,2,3,4-tetrahydroisoquinolin-1-yl)propan-2-one (3i)**

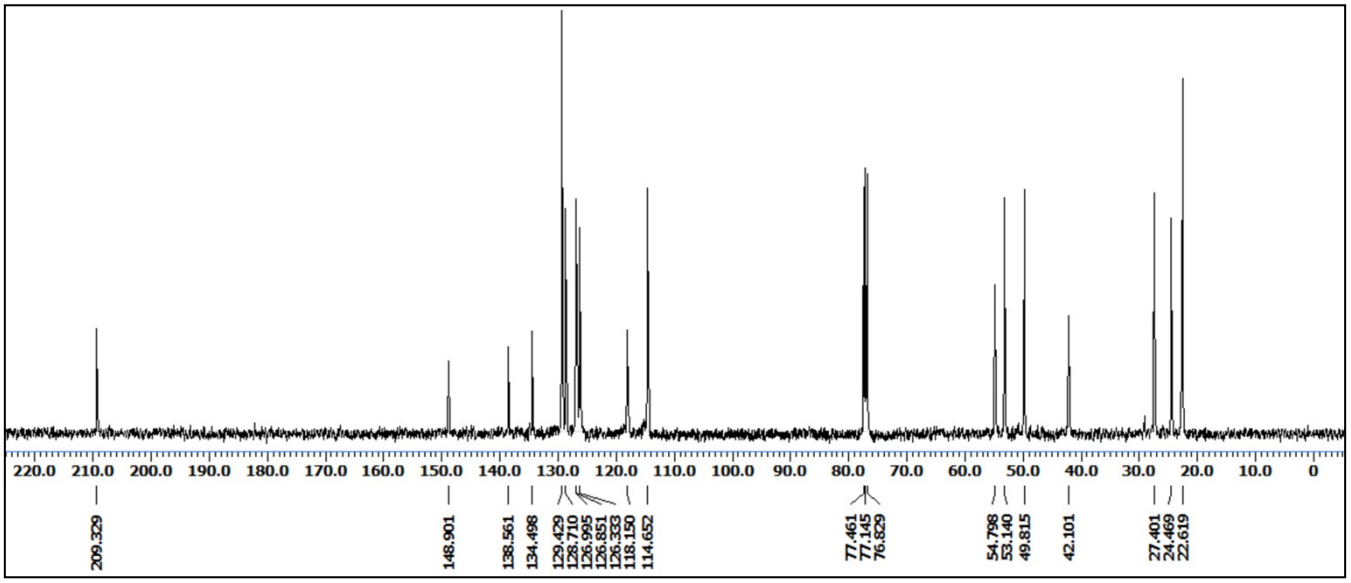

**$^{1}$H NMR**

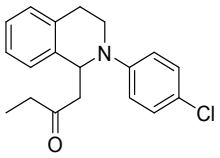


**1-(2-(4-chlorophenyl)-1,2,3,4-tetrahydroisoquinolin-1-yl)butan-2-one (3j)**

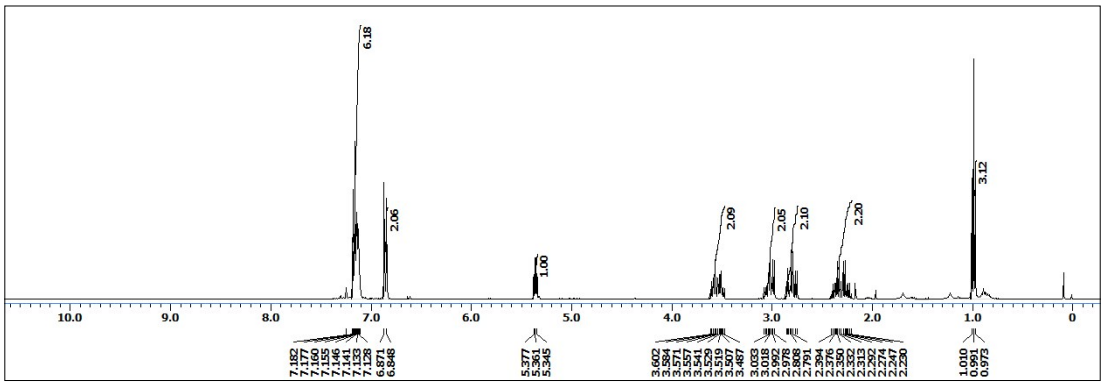


**$^{13}$C NMR**

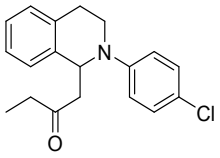


**1-(2-(4-chlorophenyl)-1,2,3,4-tetrahydroisoquinolin-1-yl)butan-2-one (3j)**

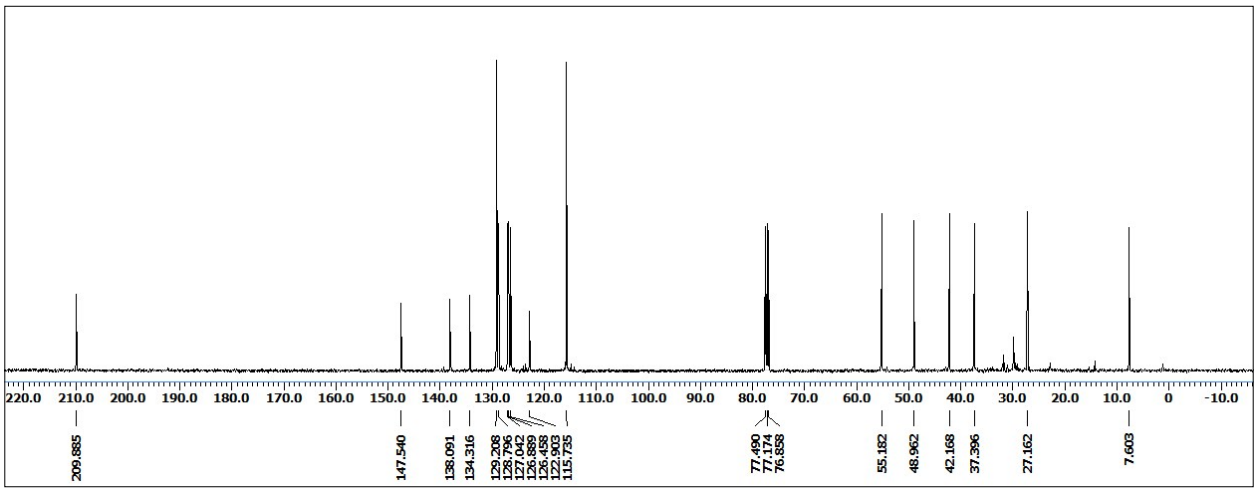

**$^{1}$H NMR**

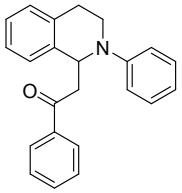

**1-Phenyl-2-(2-phenyl-1,2,3,4-tetrahydroisoquinolin-1-yl)ethan-1-one (3k)**

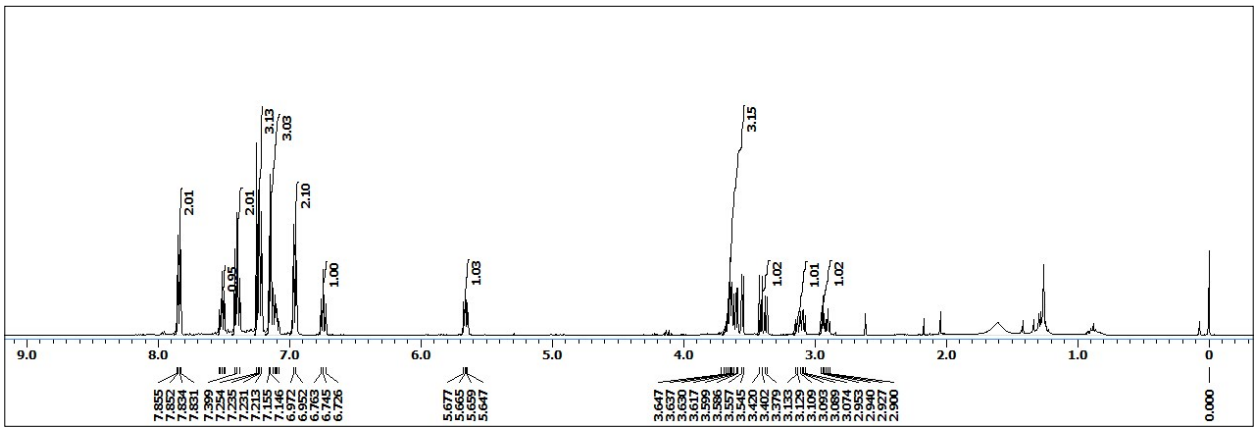

**$^{13}$C NMR**

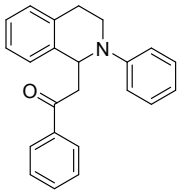

**1-Phenyl-2-(2-phenyl-1,2,3,4-tetrahydroisoquinolin-1-yl)ethan-1-one (3k)**

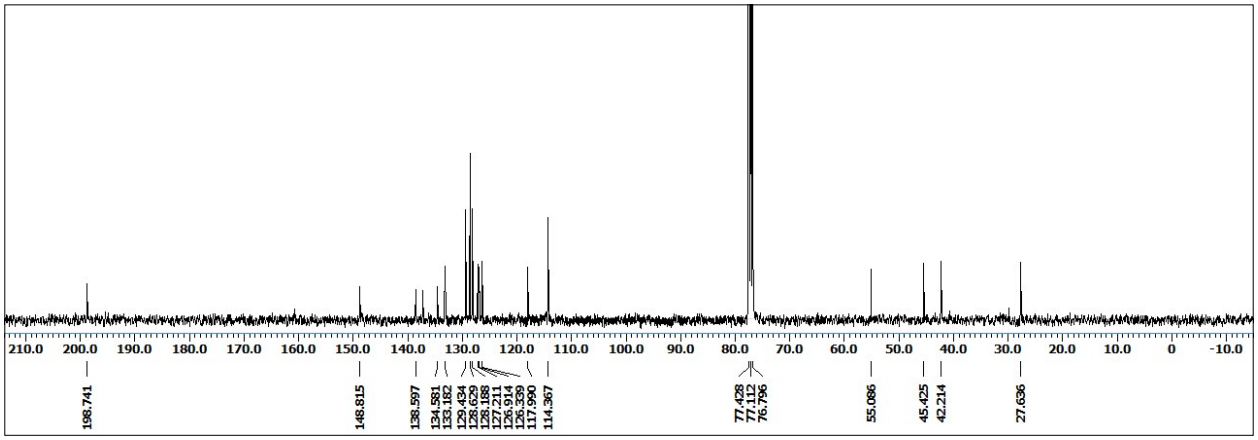

**$^{1}$H NMR**

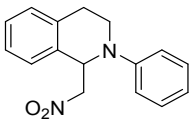


**1-(nitromethyl)-2-phenyl-1,2,3,4-tetrahydroisoquinoline (5a)**

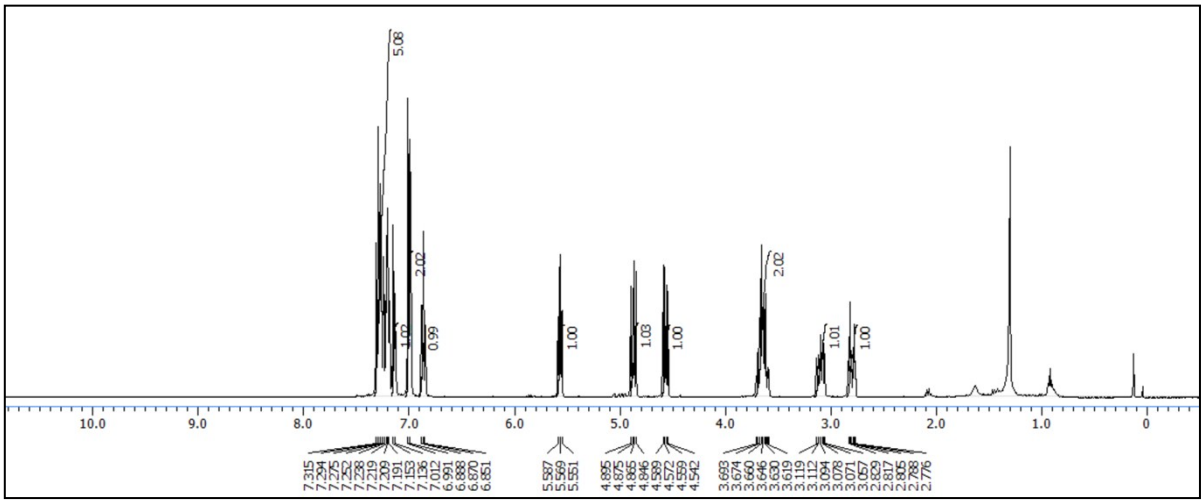


**$^{13}$C NMR**

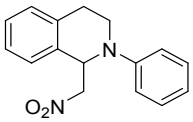


**1-(nitromethyl)-2-phenyl-1,2,3,4-tetrahydroisoquinoline (5a)**

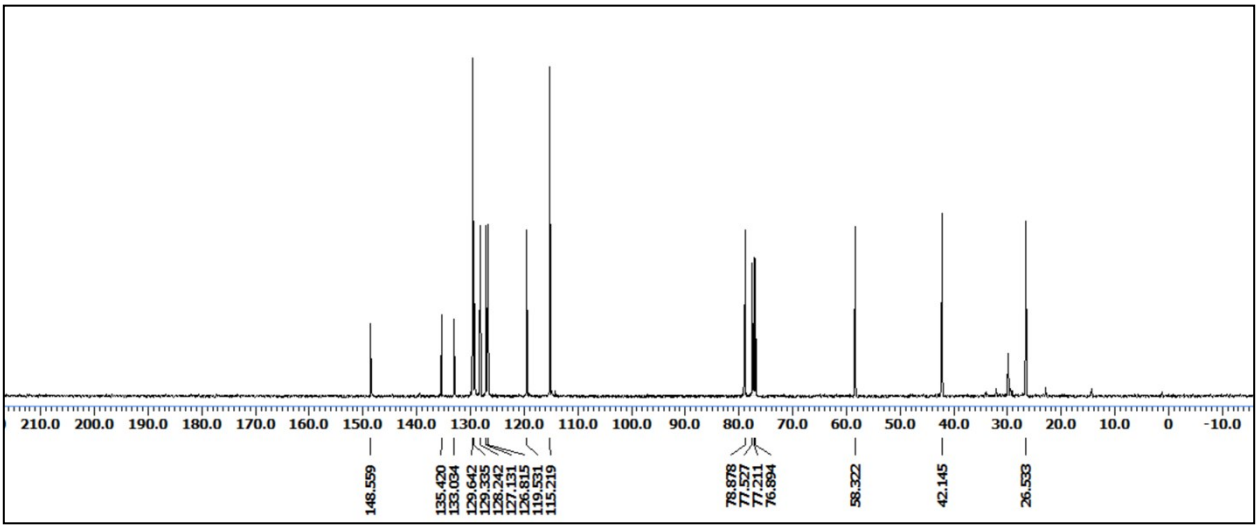

**$^{1}$H NMR**

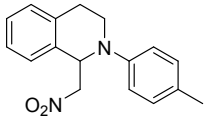


**1-(nitromethyl)-2-(p-tolyl)-1,2,3,4-tetrahydroisoquinoline (5b)**

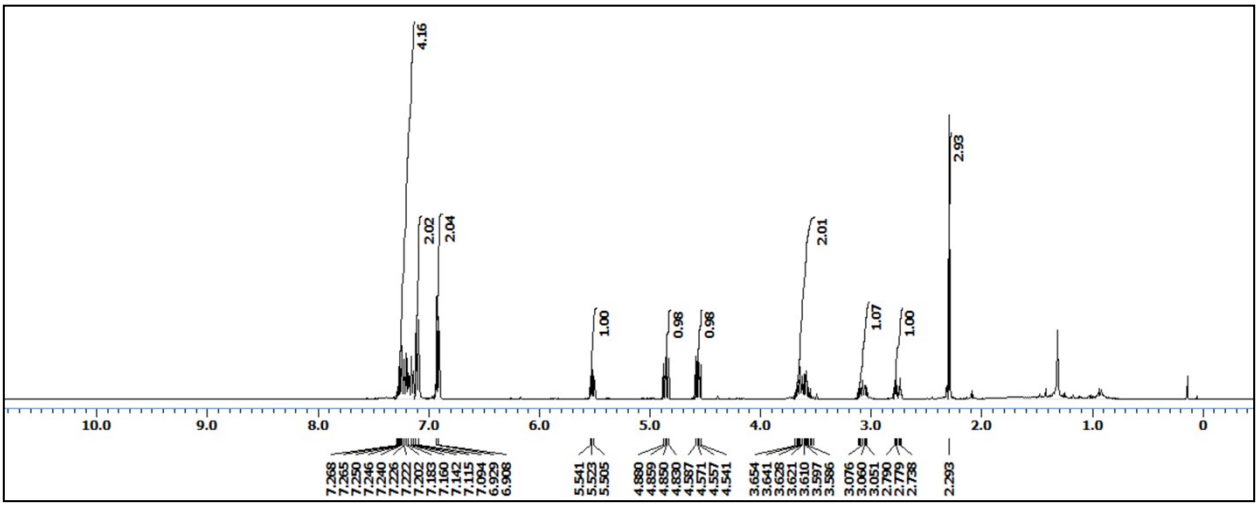


**$^{13}$C NMR**

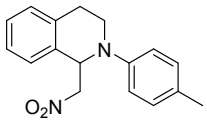


**1-(nitromethyl)-2-(p-tolyl)-1,2,3,4-tetrahydroisoquinoline (5b)**

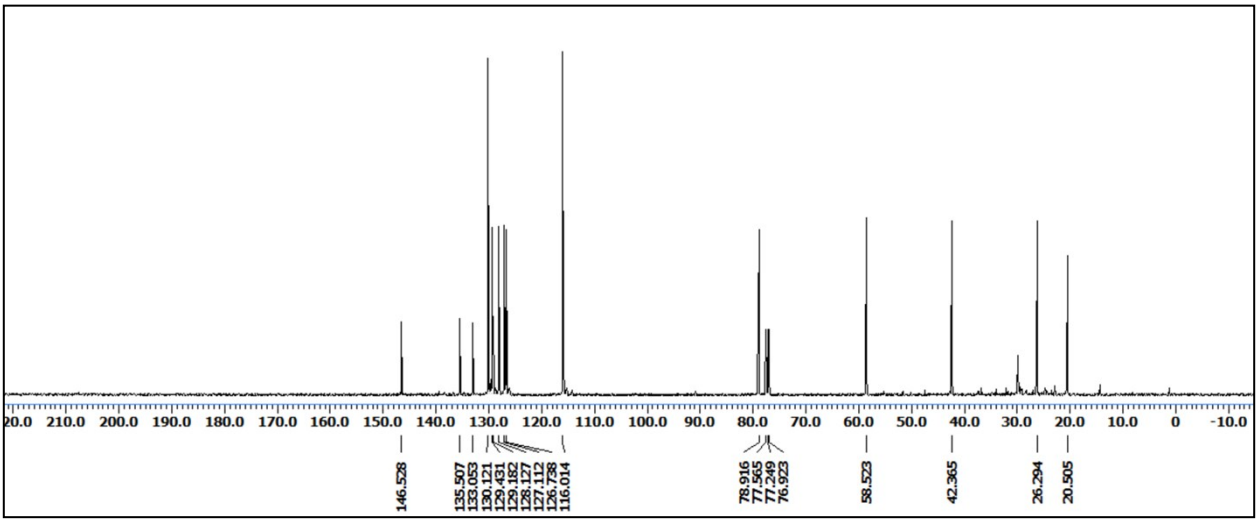

**$^{1}$H NMR**

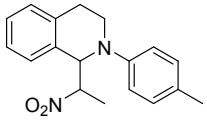

**1-(1-nitroethyl)-2-(p-tolyl)-1,2,3,4-tetrahydroisoquinoline (5c)**

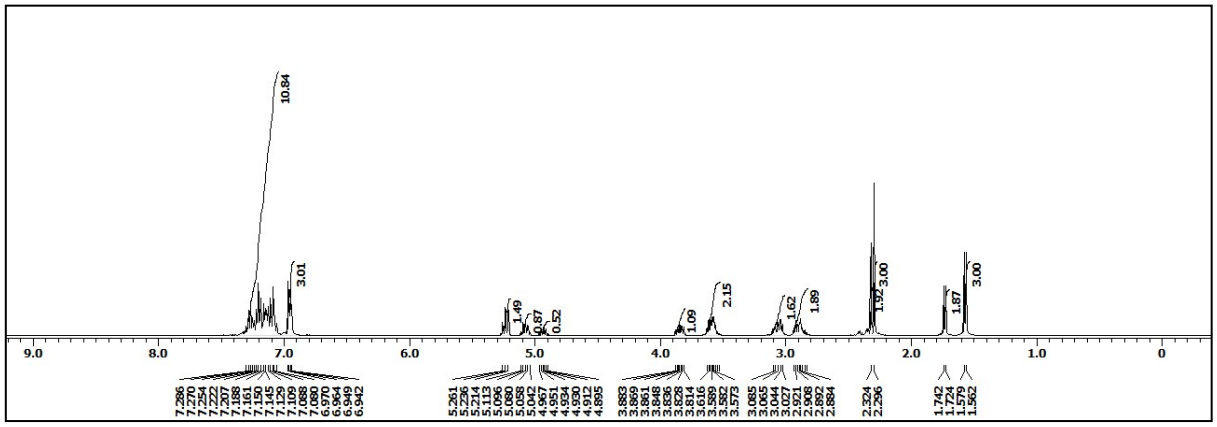

**$^{13}$C NMR**

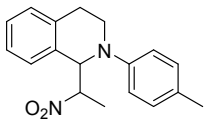

**1-(1-nitroethyl)-2-(p-tolyl)-1,2,3,4-tetrahydroisoquinoline (5c)**

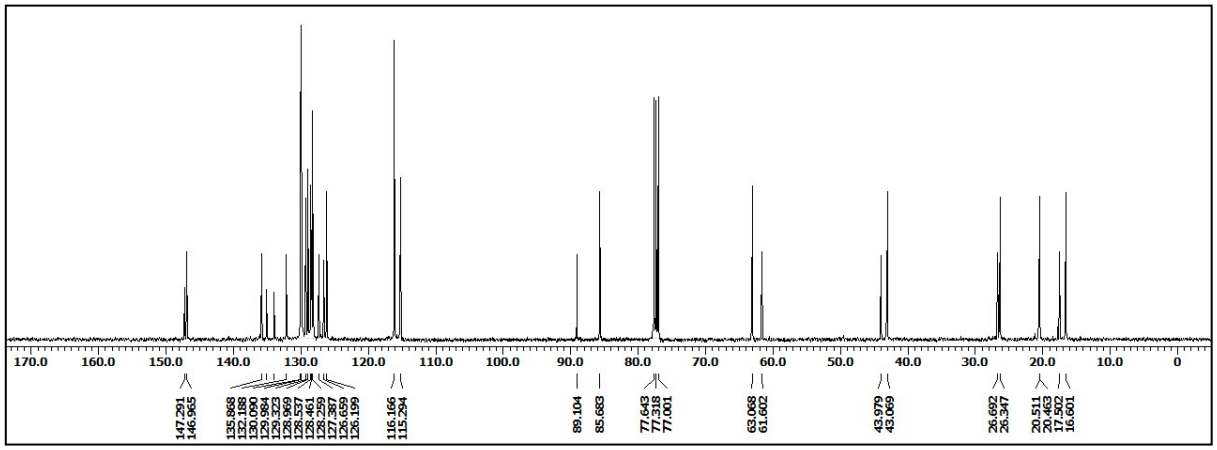

**$^{1}$H NMR**

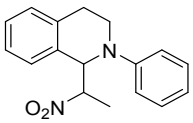


**1-(1-nitroethyl)-2-phenyl-1,2,3,4-tetrahydroisoquinoline (5d)**

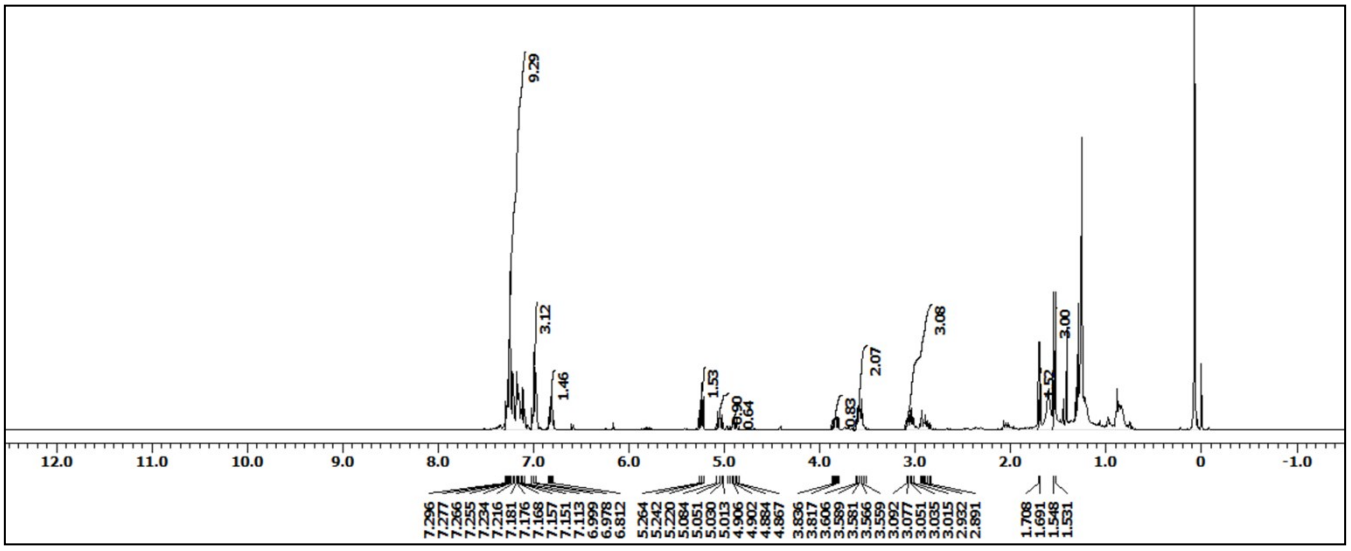


**$^{13}$C NMR**

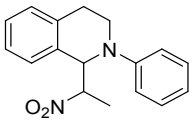


**1-(1-nitroethyl)-2-phenyl-1,2,3,4-tetrahydroisoquinoline (5d)**

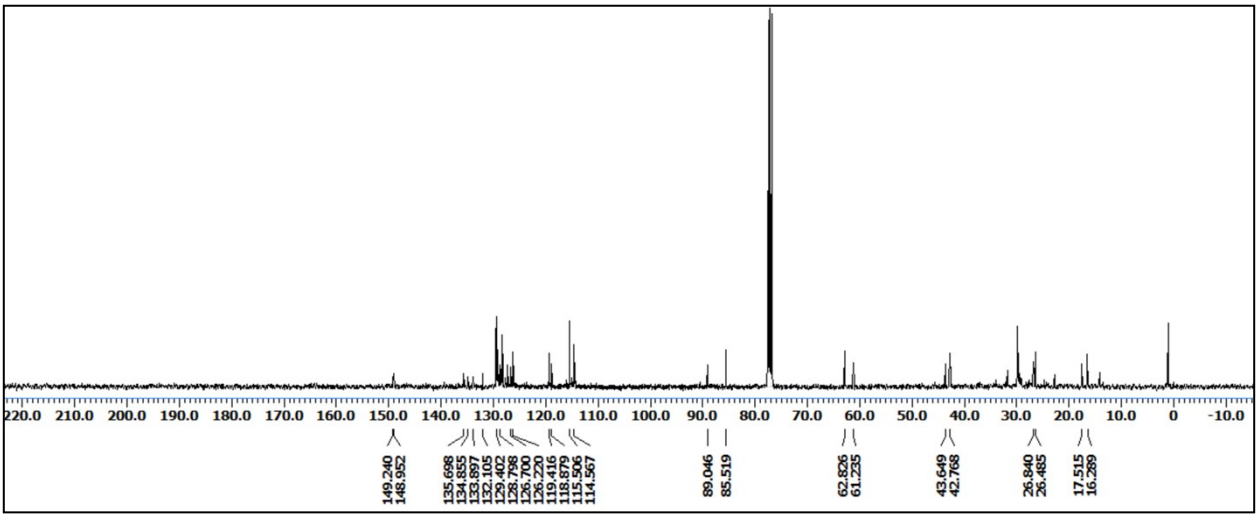

**$^{1}$H NMR**

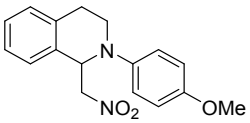


**2-(4-methoxyphenyl)-1-(nitromethyl)-1,2,3,4-tetrahydroisoquinoline (5e)**

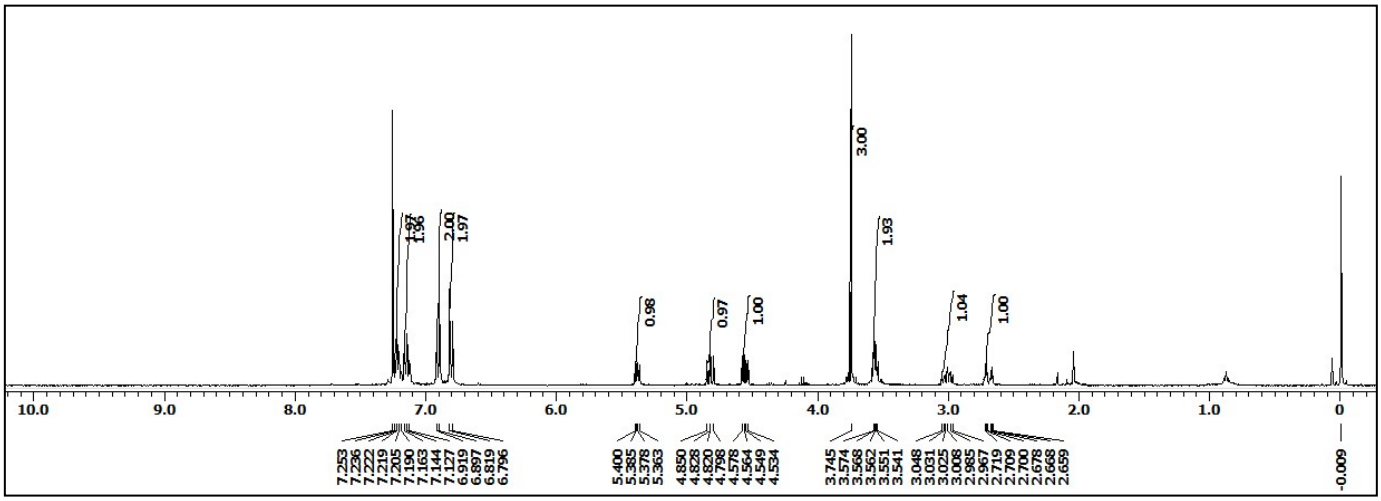


**$^{13}$C NMR**

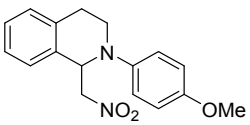


**2-(4-methoxyphenyl)-1-(nitromethyl)-1,2,3,4-tetrahydroisoquinoline (5e)**

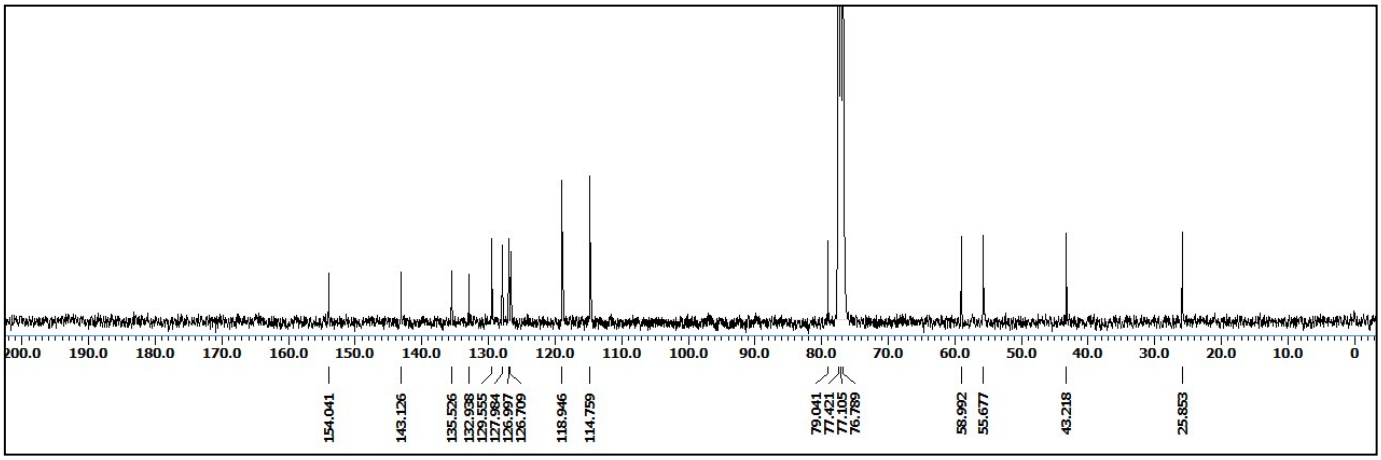

**$^1$H NMR**

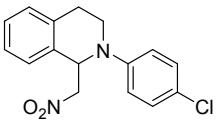


**2-(4-chlorophenyl)-1-(nitromethyl)-1,2,3,4-tetrahydroisoquinoline (5f)**

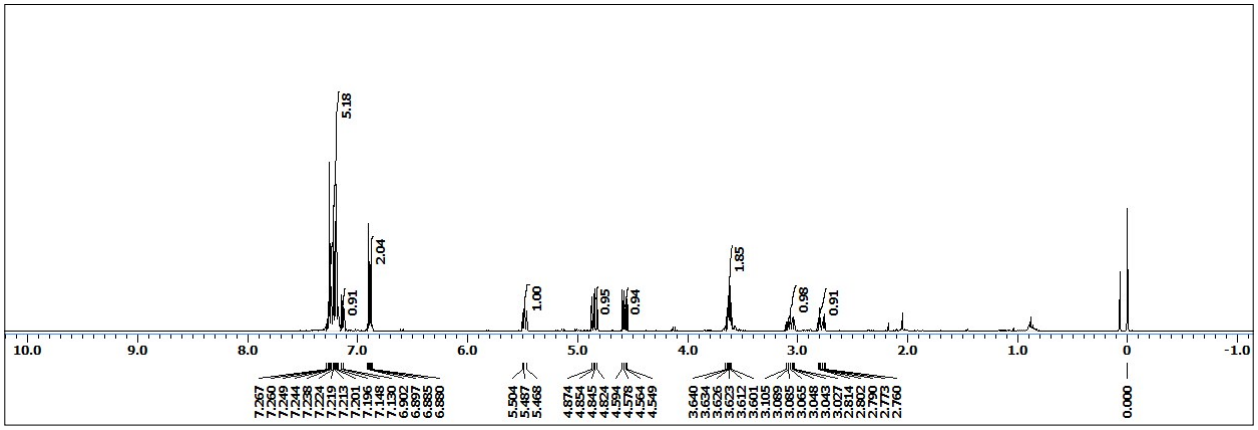


**$^{13}$C NMR**

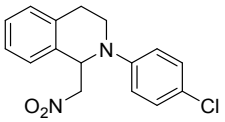


**2-(4-chlorophenyl)-1-(nitromethyl)-1,2,3,4-tetrahydroisoquinoline (5f)**

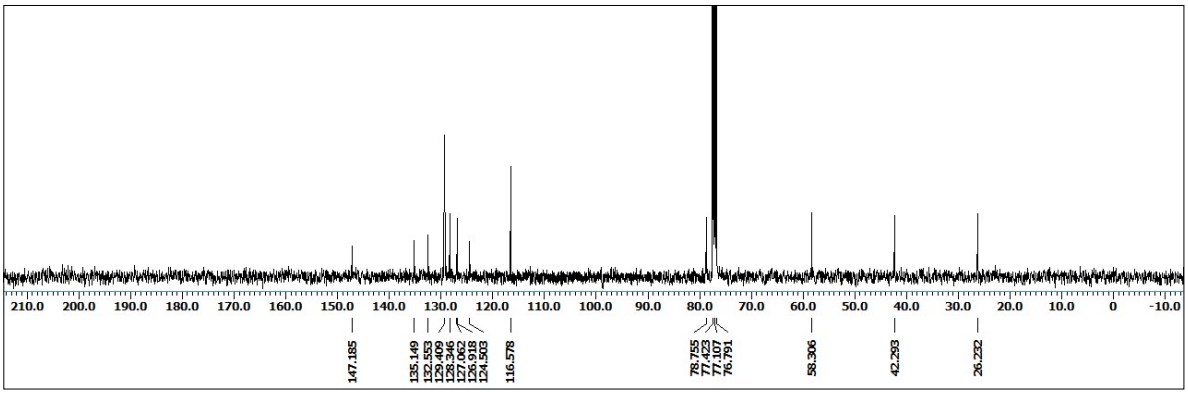


## References


1. S.-X. Lin, G.-J. Sun and Q. Kang, *Chemical Communications*, 2017, **53**, 7665-7668.
2. R. K. Sharma, M. Yadav, R. Gaur, Y. Monga and A. Adholeya, *Catalysis Science & Technology*, 2015, **5**, 2728-2740.
3. R. K. Sharma, M. Yadav, Y. Monga, R. Gaur, A. Adholeya, R. Zboril, R. S. Varma and M. B. Gawande, *ACS Sustainable Chemistry & Engineering*, 2016, **4**, 1123-1130.
4. R. Gupta, M. Yadav, R. Gaur, G. Arora and R. K. Sharma, *Green Chemistry*, 2017, **19**, 3801-3812.
5. S. Dutta, S. Sharma, A. Sharma and R. K. Sharma, *ACS Omega*, 2017, **2**, 2778-2791.

6. I. Eckhard and L. Summers, *Australian Journal of Chemistry*, 1973, **26**, 2727-2728.
7. A. Jana, J. Mondal, P. Borah, S. Mondal, A. Bhaumik and Y. Zhao, *Chemical Communications*, 2015, **51**, 10746-10749.
8. P. Kumar, C. Joshi, N. Labhsetwar, R. Boukherroub and S. L. Jain, *Nanoscale*, 2015, **7**, 15258-15267.
9. M. Rueping, C. Vila, R. M. Koenigs, K. Poscharny and D. C. Fabry, *Chemical Communications*, 2011, **47**, 2360-2362.
10. X. Li, Y. Li, Y. Huang, T. Zhang, Y. Liu, B. Yang, C. He, X. Zhou and J. Zhang, *Green Chemistry*, 2017, **19**, 2925-2930.
11. H. E. Ho, Y. Ishikawa, N. Asao, Y. Yamamoto and T. Jin, *Chemical Communications*, 2015, **51**, 12764-12767.
12. M. Cherevatskaya, M. Neumann, S. Füldner, C. Harlander, S. Kümmel, S. Dankesreiter, A. Pfitzner, K. Zeitler and B. König, *Angewandte Chemie International Edition*, 2012, **51**, 4062-4066.
13. M. Rueping, J. Zoller, D. C. Fabry, K. Poscharny, R. M. Koenigs, T. E. Weirich and J. Mayer, *Chemistry–A European Journal*, 2012, **18**, 3478-3481.
14. J. A. Johnson, J. Luo, X. Zhang, Y.-S. Chen, M. D. Morton, E. Echeverría, F. E. Torres and J. Zhang, *ACS Catalysis*, 2015, **5**, 5283-5291.
15. L. Moehlmann, M. Baar, J. Rieß, M. Antonietti, X. Wang and S. Blechert, *Advanced Synthesis & Catalysis*, 2012, **354**, 1909-1913.
16. Y. Zhi, Z. Li, X. Feng, H. Xia, Y. Zhang, Z. Shi, Y. Mu and X. Liu, *Journal of Materials Chemistry A*, 2017, **5**, 22933-22938.